RAIRO-Oper. Res. 58 (2024) 4093–4117
https://doi.org/10.1051/ro/2024147

RAIRO Operations Research
www.rairo-ro.org

A DELAY DIFFERENTIAL EQUATION MODEL ON COVID-19 WITH VACCINATION STRATEGY

Gaurang Sharma[1,*], Amit Sharma[1] and Nishant Parmar[2]

Abstract. In this paper, we have extended SEIR model of COVID-19. The model incorporates two vital aspects in the form of vaccine compartment and constant time delay. The vaccination and time delay provide the information about immune protection and actual existence of the infection among the individuals, respectively. The model is analysed numerically and numerical simulation are executed for three different initial histories and constant time delays which affirm the biological relevance of the system. The analysis includes disease-free equilibrium (DFE), endemic equilibrium, and the basic reproduction number. The stability analysis is performed which reveal the asymptotic stability of the DFE when the basic reproduction number $R_0 < 1$. The study addresses the boundedness and positivity of the solution as the time delay approaches zero. In addition, sensitivity analysis and contour plots for R_0 with different parameters offer deeper insights into the model. The impact of vaccination and vaccine inefficacy on the model dynamics is explored.

Mathematics Subject Classification. 34A34, 49K40, 93A30, 92B05.

Received December 3, 2023. Accepted July 14, 2024.

1. Introduction

The study of existing biological systems has made extensive use of mathematical models which is very useful to unravel their complexity and for better insight to understand the problem [10, 18, 26]. Now-a-days, the most threatening existing problem to the humanity is severe acute respiratory syndrome coronavirus 2 (SARS-CoV-2). Some dynamical systems have been explored with the help of partial differential equations where some of them have been implemented directly to trace the current epidemic and provide the optimal solution against the COVID-19 battle [4, 14, 21, 27]. In view of vaccination, several models have been employed to understand optimal vaccination strategies and vaccination effects on the pandemic [7, 11, 20, 39, 41].

Further, the time delay provides the actual situation of any disease and can be helpful to make strategies to prevent the infection among the individuals. In view of COVID-19 infectious disease, it has been observed that the infection spreads step by step [25]. The breakout of infection took some time among the individuals *i.e.*, every compartment took some time to enter in another compartment. To understand the situation of such type

Keywords. Mathematical modeling, delay differential equations, COVID-19, vaccination, stability analysis, sensitivity analysis.

[1] Department of Mathematics, Shri P.N. Pandya Arts, M.P. Pandya Science & Smt. D.P. Pandya Commerce College Lunawada-389230, Shri Govind Guru University, Godhra 388713, Gujarat, India.

[2] Department of Mathematics, Government Science College, Chhotaudepur 391165, Shri Govind Guru University, Godhra 388713, Gujarat, India.

*Corresponding author: gaurangsharma508@gmail.com

of the infections, there is a great need to analyse the actual existence of the infection among the individuals. Thus, the delay differential equations play the important role to understand the current situation of infection and provide the solution in a good way. There are some mathematical models where delays impacts have been shown extensively. These existing models provide the valuable and actual information about the infection among the individuals as the delay arise in the system due to incubation periods and related phenomena. Such information has been widely implemented to make the strategies against the spread of infection across the globe. Thus, the dynamics of COVID-19 infectious disease along with time delay are reported in the literature where the target cell ACE2 receptor works as mediator during infection process [36]. In terms of ordinary and partial differential equations framework, a model on delay provides the better insights with the inclusion of spatial and temporal resolution [22].

Further, in view of vaccination strategy adopted by the government across the globe, some work follows to cure the disease and to mitigate the infection. A distributed-delay differential equation disease spread model is introduced to provide the immunity after adopting time-dependent vaccination drive [48]. In view of convex incidence rate, a delay SEIR model emphasizes the more realistic situation of infection among the individuals. The obtained results are very much promising and reveals the mitigation of the disease in near future [8]. A different and unique approach, the time delay in vaccine production, manifested the significance of vaccination rate. It is also revealed that less efficacy of vaccines is not fruitful as it will never reduce the infection among the individuals [3]. A model on time delay fractional system is established with the help of applications of fixed point theory. The authors have analysed the role of time delay in the corona virus epidemic by the graphical simulations [29]. Further, in view of constant time delay and time-discrete delay, some dynamical systems are developed with the adaptation of vaccination strategy and quarantine strategy [23, 32, 54, 60, 63].

In addition, the symptomatic-compartment along with single constant time delay and two delays are introduced to explore the current infection where sensitivity, stability and hopf bifurcation study provide the better insight of the disease [9, 35, 50, 61].

However, it has been observed that the delay in adaptation of vaccination strategy imposed serious consequences which may lead to increase in mortality of any nation by the current pandemic [5, 40]. Now-a-days, the adaptation of vaccination strategy with two doses has been implemented across the globe to get rid of the infection and to generate the immunity among the individuals [2, 19, 30, 40, 46, 49, 59].

In Indonesia, some socioeconomic and geographic disparities is followed for first and second dose of COVID-19 vaccinations [40]. Some researcher emanates the time delay with positive feedback mechanism from rejuvenate to disperse of the antibodies after vaccination drive [2, 59].

The vaccination regimen of four week has been considered as a standard time gap of vaccination between the two doses to generate the immunity in a large scale [19].

Regarding extensive delays, a dynamic model is reported in the literature to obtain the distributions of the recovered and decease periods after dividing the publicly available database into numerous subgroups. In this view, publicly available database has been separated into three groups as the total cases into 14 groups, the recovered cases into 406 groups, and the death toll into 406 groups [45]. Further, a new approach has been discussed to overcome the shortcomings of existing SEIR based models by incorporating delay differential equation's and authors claimed that the currently develop model is different from the existing most SEIR models by differentiating between tested and non-tested infected subjects [28].

In this paper, we have focused on constant time-delay to develop SEIHQRV (susceptible-exposed-infected-hospitalized-quarantined-recovered-vaccinated) model to understand the actual situation of COVID-19 disease. It has been observed that the infection spreads step by step and the breakout of infection took some time among the individuals. Thus, the delay differential equations can be useful to understand the current situation of infection among the individuals. In view of the design of this paper, the following sections have been compiled as follows: The general introduction about the pandemic is dictated in Section 1. The construction of the mathematical model is provided in the Section 2. The model is analysed in Section 3 where invariant region for positivity and boundedness of solution, both disease free and endemic equilibrium points, basic reproduction number and local stability have been performed. The numerical simulation is provided successfully of the

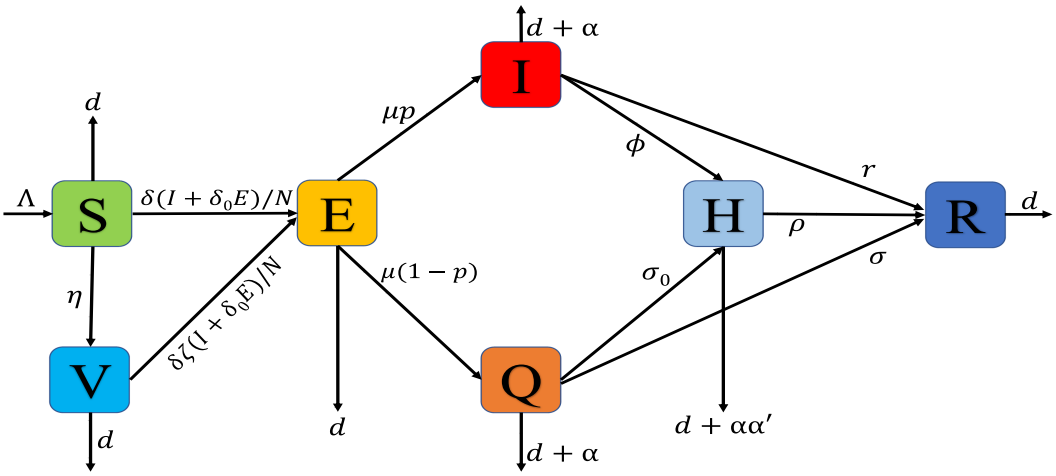

FIGURE 1. Schematic diagram of the model system (1).

TABLE 1. Nomenclature of parameters used in the model.

Parameters	Meaning	Value	Reference
Λ	Recruitment rate	0.09	[51]
δ	Disease transmission rate from susceptible to infected individuals	0.3766	Estimated
δ_0	Reduction in disease transmission for exposed individuals	0.2	[53]
d	Natural death rate	0.2516	[1]
μ	Rate at which exposed individuals leaving exposed class to infected class	1/(5.1)	[15]
p	Fraction of exposed class joining infected class	0.95	[55]
α	Disease related death rate	0.0175	[6, 53]
$\alpha^{'}$	Reduction in disease induced mortality for hospitalized individuals	0.1	[55]
r	Recovery rate for infected class	1/14	[6]
ϕ	Rate at which infected individuals admitted to hospitals	0.2174	[31]
ρ	Recovery rate of hospitalized individuals	0.32772	[3]
σ	Recovery rate of quarantine individuals	0.1162	[56]
σ_0	Rate by which quarantine individuals become infected	0.1429	[53]
η	Vaccination rate	0.5	[62]
ζ	Disease exposure rate for vaccinated individuals (Vaccine inefficacy)	0.08	[62]
N	Total population	1	Fixed

proposed model and presented in Section 4. In Section 5, the sensitivity analysis is performed for the threshold quantity R_0, and the contour plots reveal the variation in R_0 with respect to different values of the various parameters involved in the model. Finally, conclusions are appended in the Section 6.

2. Model formulation

The constant time delay is incorporated in the model formulation to know the actual situation of COVID-19 disease. The total population N is divided into seven compartments as susceptible $S(t)$, exposed $E(t)$, infected $I(t)$, hospitalized $H(t)$, quarantined $Q(t)$, recovered $R(t)$ & vaccinated $V(t)$.

Figure 1 represents the dynamics of the mathematical model.

Further, the following system of differential equations with delay is deduced based on schematic diagram 1:

$$\begin{aligned}
\frac{dS}{dt} &= \Lambda - \frac{\delta S(I+\delta_0 E)}{N} - \eta S - dS(t-\tau),\\
\frac{dE}{dt} &= \frac{\delta S(I+\delta_0 E)}{N} + \zeta V I + \frac{\delta\zeta V(I+\delta_0 E)}{N} - dE - \mu E(t-\tau),\\
\frac{dI}{dt} &= \mu p E - (d+\alpha)I - rI - \phi I,\\
\frac{dH}{dt} &= \phi I - (d+\alpha\alpha^{'})H - \rho H + \sigma_0 Q,\\
\frac{dQ}{dt} &= \mu E(t-\tau) - \mu p E - (d+\alpha)Q - \sigma Q - \sigma_0 Q,\\
\frac{dR}{dt} &= \rho H + \sigma Q - dR + rI,\\
\frac{dV}{dt} &= \eta S - \zeta V I - \frac{\delta\zeta V(I+\delta_0 E)}{N} - dV.
\end{aligned} \tag{1}$$

Where $t \in [0,\infty)$, and with initial conditions given by

$$S(\theta) = \zeta_1(\theta) > 0, E(\theta) = \zeta_2(\theta) \geq 0, I(\theta) = \zeta_3(\theta) \geq 0, H(\theta) = \zeta_4(\theta) \geq 0,$$

$$Q(\theta) = \zeta_5(\theta) \geq 0, R(\theta) = \zeta_6(\theta) \geq 0, V(\theta) = \zeta_7(\theta) \geq 0,$$

for $\theta \in [-\tau, 0]$ with $\zeta_i(\theta), i = 1,\ldots,7$ continuous functions defined from the interval $[-\tau,0]$ to R_+ and with norm $\|\zeta_i\| = sup_{-\tau\leq\theta\leq 0}|\zeta_i(\theta)|, i = 1,\ldots,7$. Let $b > 0$ and $\mathcal{S} = \mathcal{C}([-\tau,b], R_+^7)$ be the Banach space of continuous functions defined on the interval $[-\tau,b]$ to R_+^7 with the norm

$$\|x\| = sup_{-\tau\leq\theta\leq b}\|x(\theta)\|, x \in \mathcal{S},$$

where $\|x(\theta)\| = \sum_{i=1}^{7}|x_i(\theta)|$, [24].

It is evident from the literature that the infection spreads step by step and the breakout of infection took some time among the individuals [25,34,52]. Thus, to analyse the actual situation of such type of the infections, delay differential equations play the important role. The strategy can be developed perfectly based on the prediction of delay in the system.

The following parameters $\Lambda, \delta, \delta_0, d, \frac{1}{\mu}, p, \alpha, \alpha^{'}, r, \phi, \rho, \sigma, \sigma_0, \eta$ and ζ are used throughout the paper and nomenclature is provided in the Table 1.

The dynamics of the solutions of system (1) is demonstrated and total population can be bifurcated into compartments. So that it can be written as

$$N(t) = S(t) + E(t) + I(t) + H(t) + Q(t) + R(t) + V(t).$$

As per the biological behaviour, it is evident from the literature that the new recruits join susceptible class, therefore, $S(0)$ will always be greater than zero strictly, and the initial conditions of remaining class *i.e.*, $E(0), I(0), Q(0), H(0), R(0)$ and $V(0)$ are either positive or zero. Thus, the following initial conditions have been used to analyse the model:

$$S(0) > 0, E(0) \geq 0, I(0) \geq 0, H(0) \geq 0, Q(0) \geq 0, R(0) \geq 0, V(0) \geq 0. \tag{2}$$

Moreover, the following equation having constant time delays satisfy the compatibility conditions:

$$S(0) = \zeta_1(0) \quad and \quad E(0) = \zeta_2(0).$$

3. Model analysis

The model is analysed and the numerical solution is carried out to elaborate the actual infection among the individuals. In this section, we have discussed the major points like the invariant region, positivity of solution, disease free equilibrium point, endemic equilibrium point, basic reproduction number and local stability as follows:

3.1. Invariant region

In this subsection, it has been observed that the dynamic system represented in (1) have a region where the solution of the above mentioned model is uniformly bounded in the proper subset Ω of R_+^7. The following result is in support as:

Theorem 1. *The dynamic model represented in (1) with initial conditions given by (2) has positive solutions* $\big(S(t), E(t), I(t), H(t), Q(t), R(t), V(t)\big)$ *for all* $t \in [0, \infty)$*, when* $\tau \to 0^+$.

Proof. The positivity of the dynamic system (1), can be investigated with the help of vector field. So that, we have focused to elaborate the direction of the vector field of the model system (1). Thus, we have observed that:

$$\begin{aligned}
\left(\frac{dS}{dt}\right)_{S=0} &= \Lambda \geq 0,\\
\left(\frac{dE}{dt}\right)_{E=0} &= \frac{\delta SI}{N} + \zeta VI + \frac{\delta \zeta VI}{N} \geq 0,\\
\left(\frac{dI}{dt}\right)_{I=0} &= \mu pE \geq 0,\\
\left(\frac{dH}{dt}\right)_{H=0} &= \phi I + \sigma_0 Q \geq 0,\\
\left(\frac{dQ}{dt}\right)_{Q=0} &= \mu E(t-\tau) - \mu pE \geq 0,\\
\left(\frac{dR}{dt}\right)_{R=0} &= \rho H + \sigma Q + rI \geq 0,\\
\left(\frac{dV}{dt}\right)_{V=0} &= \eta S \geq 0.
\end{aligned} \tag{3}$$

It follows that R_+^7 is a positively invariant set of the SEIHQRV model system (1) for all $t \geq 0$. Thus, for non negative initial conditions, the observed non negative solution of the dynamic model emphasizes the acceptance of the theorem. □

Theorem 2. *All solutions of the proposed dynamic model system (1) are bounded.*

Proof. From the model system (1), we get

$$(S+E+I+H+Q+R+V)' = \Lambda - d(S+E+I+H+Q+R+V) - \alpha I - \alpha Q - \alpha\alpha' H,$$

which can be written as,

$$(S+E+I+H+Q+R+V)' \leq \Lambda - d(S+E+I+H+Q+R+V),$$

which gives us

$$\lim_{t\to\infty} Sup(S+E+I+H+Q+R+V) \leq \frac{\Lambda}{d}.$$

Now, from first equation of the model (1), it has been observed that

$$\frac{dS}{dt} \leq \Lambda - dS \Rightarrow S(t) \leq \frac{\Lambda}{d}.$$

Similarly, the bounds for other components of the solution can be obtained. Thus, we have obtained the feasible region (Ω) for the dynamic model system (1) as

$$\Omega = \left\{ (S, E, I, H, Q, R, V) \in R_+^7 | S + E + I + H + Q + R + V \leq \frac{\Lambda}{d} \right\},$$

which is a positively invariant set. This completes the proof. □

3.2. Disease-free equilibrium point (DFEP) and Endemic equilibrium point (EEP)

The present dynamic system admits the absence of disease among the individuals. In this sub-section, we have obtained the disease free equilibrium point as assuming all the right hand sides of (1) to zero and $I = E = 0$, *i.e.*,

$$\begin{aligned}
\Lambda - \frac{\delta S(I + \delta_0 E)}{N} - \eta S - dS(t-\tau) &= 0,\\
\frac{\delta S(I + \delta_0 E)}{N} + \zeta V I + \frac{\delta \zeta V(I + \delta_0 E)}{N} - dE - \mu E(t-\tau) &= 0,\\
\mu p E - (d + \alpha) I - rI - \phi I &= 0,\\
\phi I - (d + \alpha\alpha^{'}) H - \rho H + \sigma_0 Q &= 0,\\
\mu E(t-\tau) - \mu p E - (d + \alpha) Q - \sigma Q - \sigma_0 Q &= 0,\\
\rho H + \sigma Q - dR + rI &= 0,\\
\eta S - \zeta V I - \frac{\delta \zeta V(I + \delta_0 E)}{N} - dV &= 0.
\end{aligned} \tag{4}$$

Since,

$$\lim_{t\to\infty} S(t) = \lim_{t\to\infty} S(t-\tau),$$
$$\lim_{t\to\infty} E(t) = \lim_{t\to\infty} E(t-\tau),$$

and $I = E = 0$, we get,

$$S^0 = \frac{\Lambda}{d+\eta}, V^0 = \frac{\Lambda\eta}{d(d+\eta)}.$$

Therefore, DFE can be demonstrated as,

$$X^0 = (S^0, E^0, I^0, H^0, Q^0, R^0, V^0) = \left(\frac{\Lambda}{d+\eta}, 0, 0, 0, 0, 0, \frac{\Lambda\eta}{d(d+\eta)} \right),$$

which represents the disease free state or there is no infection among the individuals. For endemic equilibrium, we have $X^* = (S^*, E^*, I^*, H^*, Q^*, R^*, V^*)$, where,

$$\begin{aligned}
S^* &= \frac{\Lambda}{d + \eta + \frac{\delta\left(I^* + \frac{I^*\,\delta_0\,(\alpha+d+\phi+r)}{\mu\, p}\right)}{N}},\\
E^* &= \frac{I^*\,(\alpha + d + \phi + r)}{\mu\, p},\\
I^* &> 0,
\end{aligned}$$

$$H^* = \frac{I^*\,\phi - \frac{\sigma_0\left(I^*\,(\alpha+d+\phi+r) - \frac{I^*\,(\alpha+d+\phi+r)}{p}\right)}{\alpha+d+\sigma+\sigma_0}}{d+\rho+\alpha\,\alpha_1},$$

$$Q^* = -\frac{I^*\,(\alpha+d+\phi+r) - \frac{I^*\,(\alpha+d+\phi+r)}{p}}{\alpha+d+\sigma+\sigma_0},$$

$$R^* = \frac{I^*\,r - \frac{\sigma\left(I^*\,(\alpha+d+\phi+r) - \frac{I^*\,(\alpha+d+\phi+r)}{p}\right)}{\alpha+d+\sigma+\sigma_0} + \frac{\rho\left(I^*\,\phi - \frac{\sigma_0\left(I^*\,(\alpha+d+\phi+r) - \frac{I^*\,(\alpha+d+\phi+r)}{p}\right)}{\alpha+d+\sigma+\sigma_0}\right)}{d+\rho+\alpha\,\alpha_1}}{d},$$

$$V^* = \frac{\Lambda\,\eta}{\left(d + I^*\,\zeta + \frac{\delta\,\zeta\left(I^* + \frac{I^*\,\delta_0\,(\alpha+d+\phi+r)}{\mu\,p}\right)}{N}\right)\left(d+\eta+\frac{\delta\left(I^* + \frac{I^*\,\delta_0\,(\alpha+d+\phi+r)}{\mu\,p}\right)}{N}\right)}.$$

3.3. Basic Reproduction Number (R_0)

Basic reproduction number of any system is one of the important aspects and several studies have been reported in the literature for estimation of the basic reproduction number (R_0) of other diseases also [37,42–44]. Further, the basic reproduction number, R_0, can be depicted as the average number of new infections generated after the interaction of infected individuals with susceptible individuals. For the current disease COVID-19 and owing the importance of basic reproduction number, some studies have been stated the prediction of the current pandemic. The next generation matrix approach has been taken into account to find R_0 [12,13,17,33,57,58,64]. Thus, $\mathscr{F}$ and $\mathscr{V}$ are vectors as the rate of appearance of new infections and the rate of transfer of individuals out of compartments E, I, respectively. These vectors form the matrix manifested as below:

$$\mathscr{F} = \begin{bmatrix} \frac{\delta S(I+\delta_0 E)}{N} + \zeta V I + \frac{\delta\zeta V(I+\delta_0 E)}{N} \\ 0 \end{bmatrix},$$

$$\mathscr{V} = \begin{bmatrix} dE + \mu E \\ -(\mu p E) + (d+\alpha+r+\phi)I \end{bmatrix}.$$

Therefore, we have obtained the matrices F and V as the Jacobian matrices evaluated at the disease free point X^0, as follows:

$$F = \begin{bmatrix} \frac{\Lambda\,\delta\,\delta_0}{N^0\,(d+\eta)} + \frac{\Lambda\,\delta\,\delta_0\,\eta\,\zeta}{N^0\,d\,(d+\eta)} & \frac{\Lambda\,\delta}{N^0\,(d+\eta)} + \frac{\Lambda\,\eta\,\zeta}{d\,(d+\eta)} + \frac{\Lambda\,\delta\,\eta\,\zeta}{N^0\,d\,(d+\eta)} \\ 0 & 0, \end{bmatrix},$$

$$V = \begin{bmatrix} d+\mu & 0 \\ -\mu p & d+\alpha+r+\phi \end{bmatrix},$$

where, $N^0 = S^0 + V^0$.
Thus, the inverse of V is

$$V^{-1} = \begin{bmatrix} \frac{1}{d+\mu} & 0 \\ \frac{\mu\,p}{(d+\mu)\,(\alpha+d+\phi+r)} & \frac{1}{\alpha+d+\phi+r} \end{bmatrix}.$$

Next, one obtains that

$$FV^{-1} = \begin{bmatrix} \frac{\Lambda\,\delta\,\delta_0}{N^0\,(d+\eta)} + \frac{\Lambda\,\delta\,\delta_0\,\eta\,\zeta}{N^0\,d\,(d+\eta)} & \frac{\Lambda\,\delta}{N^0\,(d+\eta)} + \frac{\Lambda\,\eta\,\zeta}{d\,(d+\eta)} + \frac{\Lambda\,\delta\,\eta\,\zeta}{N^0\,d\,(d+\eta)} \\ \frac{\mu\,p\left(\frac{\Lambda\,\delta}{N^0\,(d+\eta)} + \frac{\Lambda\,\eta\,\zeta}{d\,(d+\eta)} + \frac{\Lambda\,\delta\,\eta\,\zeta}{N^0\,d\,(d+\eta)}\right)}{(d+\mu)\,(\alpha+d+\phi+r)} & \frac{\Lambda\,\delta}{N^0\,(d+\eta)} + \frac{\Lambda\,\eta\,\zeta}{d\,(d+\eta)} + \frac{\Lambda\,\delta\,\eta\,\zeta}{N^0\,d\,(d+\eta)} \\ 0 & 0 \end{bmatrix}.$$

R_0 is the spectral radius of matrix FV^{-1} of the system (1).

$$R_0 = \frac{\Lambda\,\delta\,\delta_0\,(d+\eta\,\zeta)}{N^0\,d\,(d+\eta)\,(d+\mu)} + \frac{\Lambda\,\mu\,p\,\left(d\,\delta + N^0\,\eta\,\zeta + \delta\,\eta\,\zeta\right)}{N^0\,d\,(d+\eta)\,(d+\mu)\,(\alpha+d+\phi+r)}. \tag{5}$$

3.4. Local stability of disease-free equilibrium

For disease free equilibrium, the number of infected individuals should tend to zero. Thus, the value of basic reproduction will be less than zero. So that, if $R_0 < 1$ then disease-free equilibrium of the model is considered as locally asymptotically stable.

Theorem 3. *The disease-free equilibrium X^0 is locally asymptotically stable if $R_0 < 1$, and unstable if $R_0 > 1$ for $\tau \geq 0$, where R_0 is mentioned in equation (5).*

Proof. For local stability analysis, the characteristic equation of system (1) is as follows:

$$det[\lambda I - J - e^{-\lambda\tau} J_D] = 0, \tag{6}$$

where

$$J = \begin{pmatrix} A_1 & -\frac{S\,\delta\,\delta_0}{N} & -\frac{S\,\delta}{N} & 0 & 0 & 0 & 0 \\ \frac{\delta\,(I+E\,\delta_0)}{N} & A_2 & V\,\zeta + \frac{S\,\delta}{N} + \frac{V\,\delta\,\zeta}{N} & 0 & 0 & 0 & A_5 \\ 0 & \mu\,p & -\alpha - d - \phi - r & 0 & 0 & 0 & 0 \\ 0 & 0 & \phi & A_3 & \sigma_0 & 0 & 0 \\ 0 & -\mu\,p & 0 & 0 & A_4 & 0 & 0 \\ 0 & 0 & r & \rho & \sigma & -d & 0 \\ \eta & -\frac{V\,\delta\,\delta_0\,\zeta}{N} & -V\,\zeta - \frac{V\,\delta\,\zeta}{N} & 0 & 0 & 0 & -d - A_5 \end{pmatrix},$$

where,

$$\begin{aligned} A_1 &= -\eta - \frac{\delta\,(I + E\,\delta_0)}{N}, \\ A_2 &= \frac{S\,\delta\,\delta_0}{N} - d + \frac{V\,\delta\,\delta_0\,\zeta}{N}, \\ A_3 &= -d - \rho - \alpha\,\alpha_1, \\ A_4 &= -\alpha - d - \sigma - \sigma_0, \\ A_5 &= I\,\zeta + \frac{\delta\,\zeta\,(I + E\,\delta_0)}{N}, \end{aligned}$$

and

$$J_D = \begin{pmatrix} -d & 0 & 0 & 0 & 0 & 0 & 0 \\ 0 & -\mu & 0 & 0 & 0 & 0 & 0 \\ 0 & 0 & 0 & 0 & 0 & 0 & 0 \\ 0 & 0 & 0 & 0 & 0 & 0 & 0 \\ 0 & \mu & 0 & 0 & 0 & 0 & 0 \\ 0 & 0 & 0 & 0 & 0 & 0 & 0 \\ 0 & 0 & 0 & 0 & 0 & 0 & 0 \end{pmatrix}.$$

Thus, the determinant of above mentioned equation (6) is as follows:

$$\begin{vmatrix} M_1 & \frac{S\,\delta\,\delta_0}{N} & \frac{S\,\delta}{N} & 0 & 0 & 0 & 0 \\ -\frac{\delta\,(I+E\,\delta_0)}{N} & M_2 & -V\,\zeta - \frac{S\,\delta}{N} - \frac{V\,\delta\,\zeta}{N} & 0 & 0 & 0 & -A_5 \\ 0 & -\mu\,p & \alpha + d + \lambda + \phi + r & 0 & 0 & 0 & 0 \\ 0 & 0 & -\phi & M_3 & -\sigma_0 & 0 & 0 \\ 0 & \mu\,p - \mu\,\mathrm{e}^{-\lambda\,\tau} & 0 & 0 & M_4 & 0 & 0 \\ 0 & 0 & -r & -\rho & -\sigma & d+\lambda & 0 \\ -\eta & \frac{V\,\delta\,\delta_0\,\zeta}{N} & V\,\zeta + \frac{V\,\delta\,\zeta}{N} & 0 & 0 & 0 & M_5 \end{vmatrix} = 0, \tag{7}$$

where,

$$M_1 = \lambda + d\,\mathrm{e}^{-\lambda\,\tau} - A_1,$$

$$
\begin{aligned}
M_2 &= \lambda + \mu\, \mathrm{e}^{-\lambda\,\tau} - A_2,\\
M_3 &= \lambda - A_3,\\
M_4 &= \lambda - A_4,\\
M_5 &= d + \lambda + A_5.
\end{aligned}
$$

Thus, for local stability at disease-free point $X^0 = (S^0, E^0, I^0, H^0, Q^0, R^0, V^0)$, the characteristic equation of the above mentioned equation (7) can be found as

$$
\mathrm{e}^{-2\,\lambda\,\tau}\, H\, \left(d + \eta\, \mathrm{e}^{\lambda\,\tau} + \lambda\, \mathrm{e}^{\lambda\,\tau}\right)\, \left(A_{11}\, \mathrm{e}^{\lambda\,\tau}\, \lambda^2 + \left(A_{21}\, \mathrm{e}^{\lambda\,\tau} + A_{22}\right)\, \lambda + \left(A_{31}\, \mathrm{e}^{\lambda\,\tau} + A_{32}\right)\right) = 0, \tag{8}
$$

where,

$$
\begin{aligned}
H &= (d+\lambda)^2\, (d + \lambda + \rho + \alpha\,\alpha_1)\, (\alpha + d + \lambda + \sigma + \sigma_0)\,,\\
A_{11} &= d^2 + \eta\, d,\\
A_{21} &= \alpha\, d^2 + 2\, d^2\, \eta + d^2\, \phi + d^2\, r + 2\, d^3 + \alpha\, d\, \eta + d\, \eta\, \phi + d\, \eta\, r - d^2\, \delta\, \delta_0 - d\, \delta\, \delta_0\, \eta\, \zeta,\\
A_{22} &= \mu\, d^2 + \eta\, \mu\, d,\\
A_{31} &= \alpha\, d^3 + d^3\, \eta + d^3\, \phi + d^3\, r + d^4 + \alpha\, d^2\, \eta - d^3\, \delta\, \delta_0 + d^2\, \eta\, \phi + d^2\, \eta\, r -\\
&\quad \alpha\, d^2\, \delta\, \delta_0 - d^2\, \delta\, \delta_0\, \phi - d^2\, \delta\, \delta_0\, r - d^2\, \delta\, \mu\, p - \Lambda\, \eta\, \mu\, p\, \zeta - d^2\, \delta\, \delta_0\, \eta\, \zeta -\\
&\quad \alpha\, d\, \delta\, \delta_0\, \eta\, \zeta - d\, \delta\, \delta_0\, \eta\, \phi\, \zeta - d\, \delta\, \delta_0\, \eta\, r\, \zeta - d\, \delta\, \eta\, \mu\, p\, \zeta,\\
A_{32} &= d^3\, \mu + d^2\, \mu\, \phi + d^2\, \mu\, r + \alpha\, d^2\, \mu + d^2\, \eta\, \mu + d\, \eta\, \mu\, \phi + d\, \eta\, \mu\, r + \alpha\, d\, \eta\, \mu.
\end{aligned}
$$

Here, λ denotes the eigenvalue of the system. For roots, we have two cases as follows:

1. $\tau = 0$,
2. $\tau > 0$.

Now, for $\tau = 0$, the equation (8) has roots with a negative real part and the observed eigenvalues are as follows:

$$
\begin{aligned}
\lambda_1 &= -d - \eta < 0,\\
\lambda_2 &= -\tfrac{U_1 + \sqrt{L}}{2\,(d^2 + \eta\, d)} < 0,\\
\lambda_3 &= -d - \rho - \alpha\,\alpha_1 < 0,\\
\lambda_4 &= -\alpha - d - \sigma - \sigma_0 < 0,\\
\lambda_5 &= -\tfrac{U_1 - \sqrt{L}}{2\,(d^2 + \eta\, d)} < 0,\\
\lambda_6 &= -d < 0,\\
\lambda_7 &= -d < 0,
\end{aligned} \tag{9}
$$

where U_1, and L are provided in Appendix section.

From the above equation, all the eigenvalues have negative real part, which shows that the DFE point X^0 is locally asymptotically stable.

Further, for $\tau > 0$, the roots of Equation (8) can be found as

$$
\lambda_1 = -d - \rho - \alpha\,\alpha_1 < 0, \lambda_2 = -\alpha - d - \sigma - \sigma_0 < 0, \lambda_3 = -d < 0, \lambda_4 = -d < 0.
$$

Now, for remaining roots of equation (8), we have

$$
\mathrm{e}^{-2\,\lambda\,\tau}\, \left(d + \eta\, \mathrm{e}^{\lambda\,\tau} + \lambda\, \mathrm{e}^{\lambda\,\tau}\right) = 0, \tag{10}
$$

and

$$A_{11}\,\mathrm{e}^{\lambda\,\tau}\,\lambda^2 + \left(A_{21}\,\mathrm{e}^{\lambda\,\tau} + A_{22}\right)\,\lambda + \left(A_{31}\,\mathrm{e}^{\lambda\,\tau} + A_{32}\right) = 0. \tag{11}$$

Firstly, from equation (10), we have

$$d\,\mathrm{e}^{-2\,\lambda\,\tau} + \eta\,\mathrm{e}^{-\lambda\,\tau} + \lambda\,\mathrm{e}^{-\lambda\,\tau} = 0. \tag{12}$$

Solving the above equation by multiplying $\mathrm{e}^{\lambda\,\tau}$ on both sides, we get,

$$\eta + \lambda + d\,\mathrm{e}^{-\lambda\,\tau} = 0. \tag{13}$$

Let us assume $\lambda = i\,\omega\,(\omega > 0)$ is a root of equation (13), then we have,

$$\eta + \omega\,i + d\,\mathrm{e}^{-\omega\,\tau\,i} = 0, \tag{14}$$

From Euler's formula $\mathrm{e}^{-\omega\,\tau\,i} = cos(\tau\,\omega) - isin(\tau\,\omega)$, we get,

$$\eta + \omega\,i + d\,\left(\cos\left(\omega\,\tau\right) - \,i\sin\left(\omega\,\tau\right)\right) = 0. \tag{15}$$

Distinguishing the real and imaginary parts of equation (15),

$$\eta + d\,\cos\left(\omega\,\tau\right) = 0,$$
$$\omega - d\,\sin\left(\omega\,\tau\right) = 0.$$

Then, we can get,

$$\cos\left(\omega\,\tau\right) = \frac{-\eta}{d}, \tag{16}$$
$$\sin\left(\omega\,\tau\right) = \frac{\omega}{d}. \tag{17}$$

Solving the above equations simultaneously, we have

$$\cos^2\left(\omega\,\tau\right) + \sin^2\left(\omega\,\tau\right) = \frac{\eta^2}{d^2} + \frac{\omega^2}{d^2}. \tag{18}$$

Which implies that,

$$d^2 = \eta^2 + \omega^2,$$
$$\Rightarrow \omega^2 = d^2 - \eta^2,$$
$$\Rightarrow \omega^2 = (d - \eta)\,(d + \eta).$$

Thus, we have a pair of pure imaginary roots of equation (10), so that, the stability of X^0 can change from stable to unstable.

Secondly, from equation (11), following the similar process, we have

$$A_{32} + A_{31}\,\mathrm{e}^{\omega\,\tau\,i} + \omega\,\left(A_{22} + A_{21}\,\mathrm{e}^{\omega\,\tau\,i}\right)\,i = A_{11}\,\omega^2\,\mathrm{e}^{\omega\,\tau\,i}, \tag{19}$$

where, $\lambda = i\,\omega\,(\omega > 0)$.

Now by using Euler's formula, and separating the real and imaginary parts, we have

$$-A_{11}\omega^2\cos(\omega\tau) - A_{21}\omega\sin(\omega\tau) + A_{31}\cos(\omega\tau) + A_{32} = 0,$$
$$-A_{11}\omega^2\sin(\omega\tau) + A_{21}\omega\cos(\omega\tau) + A_{31}\sin(\omega\tau) + A_{22}\omega = 0.$$

TABLE 2. Initial conditions used in the model.

Parameters	Value of IC 1	Value of IC 2	Value of IC 3
$S(\theta)$	0.9	0.6	0.3
$E(\theta)$	0.0002	0.0004	0.0006
$I(\theta)$	0.00002	0.00004	0.00006
$H(\theta)$	0	0	0
$Q(\theta)$	0	0	0
$R(\theta)$	0	0	0
$V(\theta)$	0	0	0

Which implies that,

$$\begin{aligned}\left(-A_{11}\omega^2 + A_{31}\right)\cos(\omega\tau) - A_{21}\omega\sin(\omega\tau) + A_{32} = 0,\\ \left(-A_{11}\omega^2 + +A_{31}\right)\sin(\omega\tau) + A_{21}\omega\cos(\omega\tau) + A_{22}\omega = 0.\end{aligned}$$

Then, we can get

$$\cos(\omega\tau) = -\frac{A_{31}A_{32} - A_{11}A_{32}\omega^2 + A_{21}A_{22}\omega^2}{{A_{11}}^2\omega^4 - 2A_{11}A_{31}\omega^2 + {A_{21}}^2\omega^2 + {A_{31}}^2}, \tag{20}$$

and

$$\sin(\omega\tau) = \frac{\omega\left(A_{11}A_{22}\omega^2 + A_{21}A_{32} - A_{22}A_{31}\right)}{{A_{11}}^2\omega^4 - 2A_{11}A_{31}\omega^2 + {A_{21}}^2\omega^2 + {A_{31}}^2}. \tag{21}$$

Solving the above equations simultaneously, we have

$${A_{22}}^2\omega^2 + {A_{32}}^2 = {A_{11}}^2\omega^4 - 2A_{11}A_{31}\omega^2 + {A_{21}}^2\omega^2 + {A_{31}}^2. \tag{22}$$

Thus, we have a pair of pure imaginary roots of equation (11), so that, the stability of X^0 can change from stable to unstable. This completes the proof. □

4. NUMERICAL SIMULATIONS

For simulation, the parameters values have been taken from the literature as given in Table 1. Firstly, using the values of parameters, we found that the values of all seven eigenvalues mentioned in equation (9) are $\lambda_1 = -0.7516$, $\lambda_2 = -0.6769$, $\lambda_3 = -0.5811$, $\lambda_4 = -0.5282$, $\lambda_5 = -0.2994$, $\lambda_6 = -0.2516$ and $\lambda_7 = -0.2516$, respectively. The graphical representation of eigenvalues and corresponding their eigenvectors are given in Figure 2. The red, yellow, cyan, green, black, magenta and blue dotted lines are representing eigenvectors corresponding to the eigenvalues $\lambda_1, \lambda_2, \lambda_3, \lambda_4, \lambda_5, \lambda_6$ and λ_7, respectively.

Further, the numerical simulation for the model (1) shows the agreement with the qualitative analysis results and examine the effect of some parameters. The dynamic model system (1) is solved and the numerical solution is carried out. This simulation provides the stability of the equilibrium points. Also, the numerical simulations are performed for three different initial conditions as follows, where $\theta \in [-\tau, 0]$:

The constant time delay $\tau = 120$ is taken from the literature [3]. After simulation, we found that the value of basic reproduction number is $R_0 = 0.1884 < 1$ and the value of disease free equilibrium point is $X^0 = (0.1197, 0, 0, 0, 0, 0, 0.2380)$. The Figure 3 demonstrate the solution curves of the dynamic system model with three different initial conditions along with the consideration of 2000 days for infection among the individuals. Here, we have fixed the value of time delay $\tau = 120$ days while the initial conditions have been varied which is

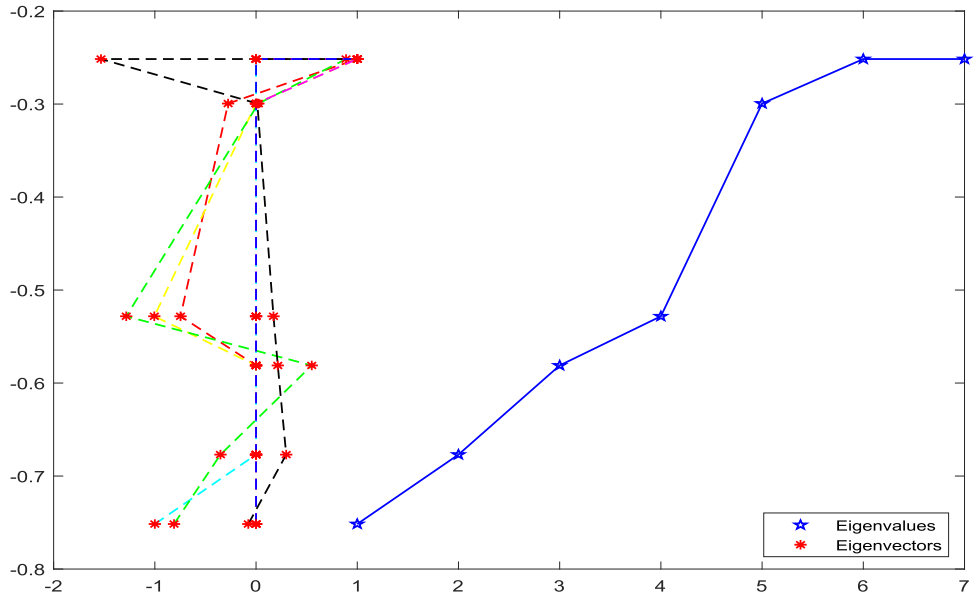

FIGURE 2. Eigenvalues and eigenvectors of the model system (1).

mentioned in Table 2. It can be seen that the susceptible, exposed, and infected individuals are in decreasing manner while hospitalized, quarantine and recovered individuals are increased first and after that decrease gradually. The vaccination individuals first decrease gradually and after that increases sharply.

Further, it is evident from the literature that the COVID-19 symptoms took some time to identify the infected individuals and some studies have shown that it takes 10-14 days approximately [45]. Thus, the constant time delay may vary and the effect of time delays has been observed. Here, we have fixed the initial condition, IC 1, and time delays τ have been varied as $\tau = 14, 16$, and 18, days. Since, delay time is taken small, so we have analysed the model for 500 days, only. Our simulation at three different time delays provides the useful information about the disease. It has been observed that oscillation of every compartment in the system increases as τ increases. Also, Figure 4 is in the support of biological behavior of the disease. Although, it has been observed that there is gradual decreasing in oscillations along with the time t.

Thus, all seven compartments of our model follow the biological behaviour of spreading of the disease among the individuals. Further, the simulation of the model depicts the non physical behaviour which can be seen in Figures 3 and 4. Eventually, the oscillatory behaviour of the model is observed as constant time delay is induced in the model. It can be perceived that increasing and decreasing in time delay τ results in the increasing and decreasing of oscillations in each compartment of the model, respectively. Thus, the large value of time delay τ leads the non physical behaviour of the model. Even more, it can be seen that all seven compartments become negative owing to the oscillations. Although, Figures 3 and 4 demonstrate the solutions of the model with non physical behaviour. It can be seen that the oscillations are smear out after some time and converge to their steady state. So that, the observed non physical behaviour does not ruin the stability of the model system (1).

The impact of vaccination on infected individuals is analysed with the parameters mentioned in Table 1. Figure 5 demonstrates that the effect of vaccination with the incorporation of different vaccination rates η and vaccine inefficacy rates ζ on the infected individuals of the model system (1). Overall, it has been observed that infection is in decreasing manner as vaccination increases. If we take the value of $\eta = 0.6$ and $\zeta = 0.07$, the size of infected individuals goes to lower level while at the value of $\eta = 0.4$ and $\zeta = 0.09$, the size of infected individuals

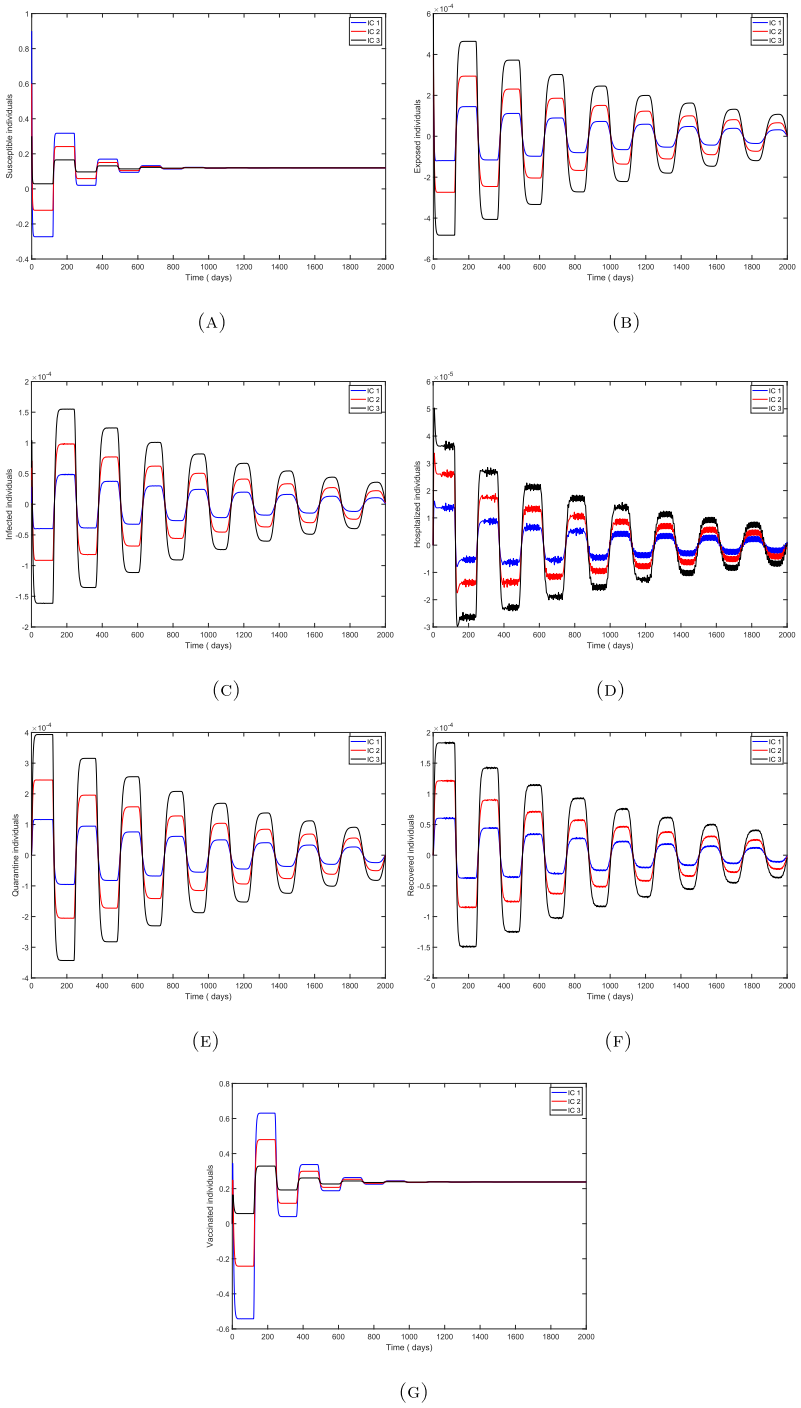

FIGURE 3. Numerical solution of model system (1) for three different initial conditions IC 1, IC 2 and IC 3. (A) Susceptible class (B) Exposed class (C) Infected class (D) hospitalized class (E) Quarantined class (F) Recovered class (G) Vaccinated class.

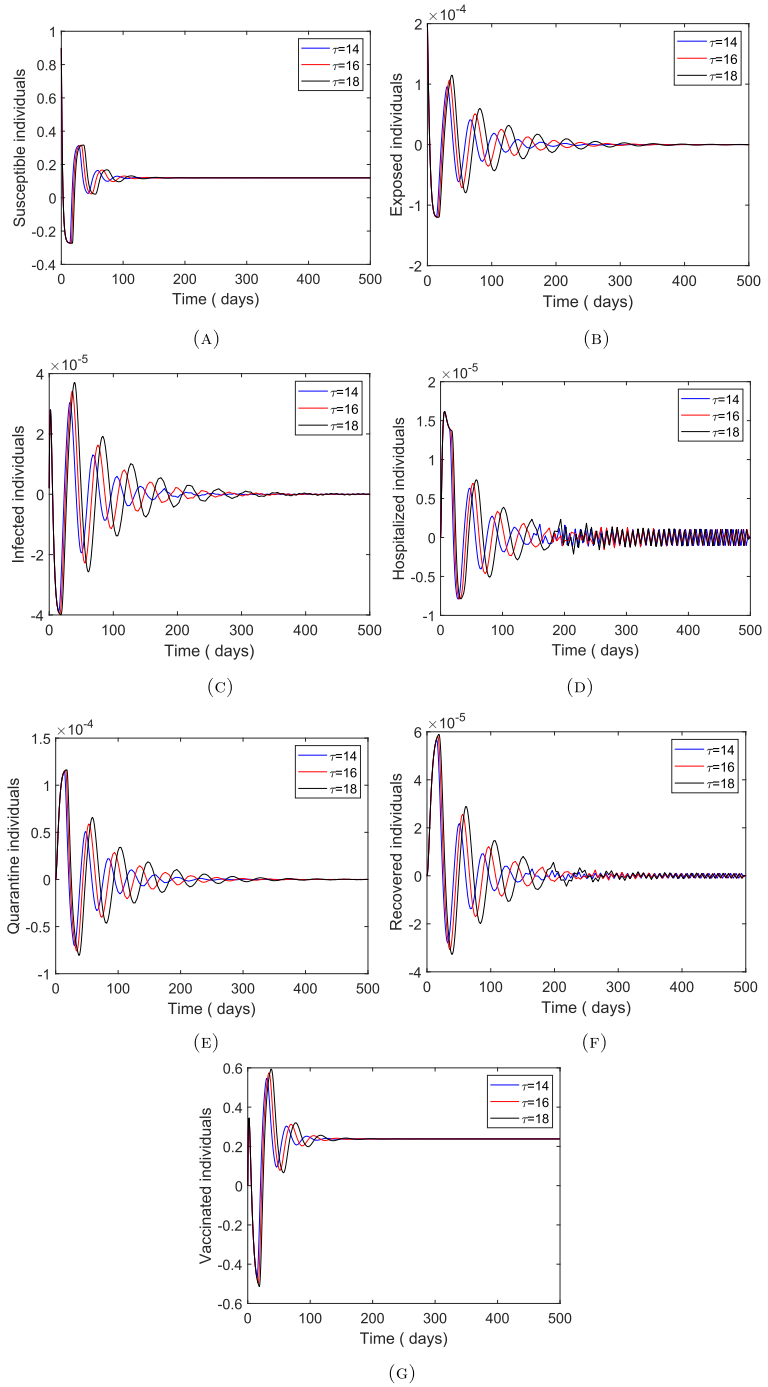

FIGURE 4. Numerical solution of model system (1) for three different constant time delays $\tau = 14, \tau = 16$ and $\tau = 18$. (A) Susceptible class (B) Exposed class (C) Infected class (D) Hospitalized class (E) Quarantined class (F) Recovered class (G) Vaccinated class.

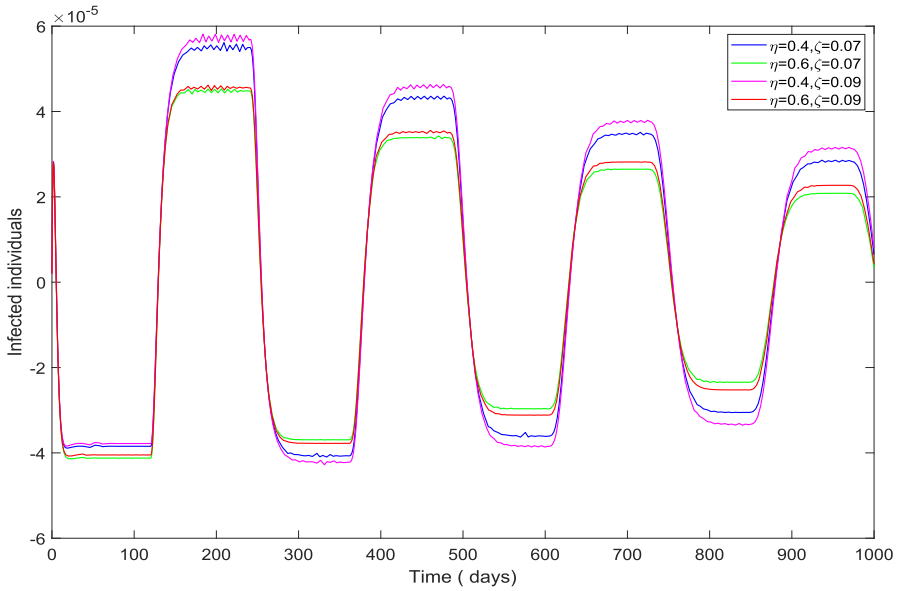

FIGURE 5. The effect of η and ζ on the infected class of the model system (1).

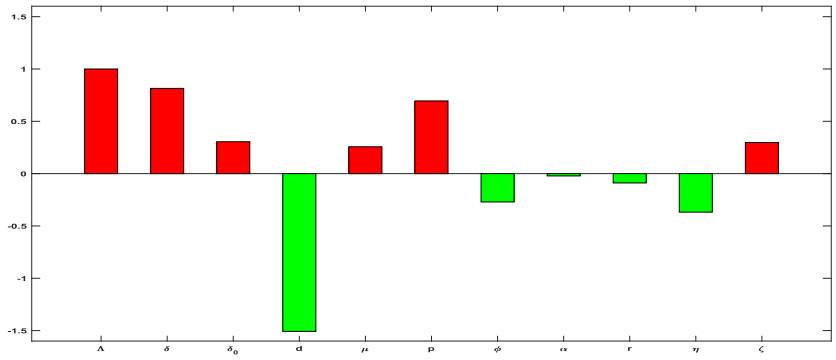

FIGURE 6. The graphical representation of the sensitivity indices of the basic reproduction number R_0 with respect to parameter $\mathcal{P}$ mentioned in Table 3 for the SEIHQRV model system (1).

goes to higher level. Thus, our study indicates that the vaccination rate and vaccination inefficacy rates should be in increasing and decreasing manner, respectively, to control the infection among the individuals.

5. Sensitivity analysis and Contour plots

The sensitivity analysis provides the outcome value of basic reproduction number R_0. It is evident from the literature that some model parameter values are not often known with certainty due to natural and seasonal variations, potential measurement errors [16, 47]. In this section, the sensitivity analysis is performed for the threshold quantity R_0, and the contour plots reveal the variation in R_0 with respect to different values of the various parameters involved in the model.

TABLE 3. The sensitivity index of basic reproduction number R_0 with respect to the parameter $\mathcal{P}$ of SEIHQRV model system (1).

Parameter $\mathcal{P}$	Meaning	Value	Sensitivity index $\prod_{R_0}^{\mathcal{P}}$
Λ	Recruitment rate	0.09	1
δ	Disease transmission rate from susceptible to infected individuals	0.3766	0.8145
δ_0	Reduction in disease transmission for exposed individuals	0.2	0.3051
d	Natural death rate	0.2516	-1.5074
μ	Rate at which exposed individuals leaving exposed class to infected class	1/(5.1)	0.2569
p	Fraction of exposed class joining infected class	0.95	0.6949
ϕ	Rate at which infected individuals admitted to hospitals	0.2174	-0.2708
α	Disease related death rate	0.0175	-0.0218
r	Recovery rate for infected class	1/14	-0.0890
η	Vaccination rate	0.5	-0.3680
ζ	Disease exposure rate for vaccinated individuals (Vaccine inefficacy)	0.08	0.2973

5.1. Sensitivity analysis for R_0

The sensitivity analysis on R_0 provides the opportunity to understand the effect of the parameters in model system (1). We perform the sensitivity analysis on R_0 with respect to the parameters and investigated as $\frac{\partial R_0}{\partial \mathcal{P}}$, where, $\mathcal{P} = (\Lambda, \delta, \delta_0, d, \mu, p, \phi, \alpha, r, \eta, \zeta)$. It is important to mitigate that R_0, for model system (1), does not depends on ρ, σ and σ_0. We found the sensitivity of R_0 to each parameter mentioned in our model system is as follows:

$$
\begin{aligned}
\frac{\partial R_0}{\partial \Lambda} &= \frac{\delta\,\delta_0\,(d+\eta\,\zeta)}{N\,d\,(d+\eta)\,(d+\mu)} + \frac{\mu\,p\,(d\,\delta + N\,\eta\,\zeta + \delta\,\eta\,\zeta)}{N\,d\,(d+\eta)\,(d+\mu)\,(\alpha+d+\phi+r)},\\
\frac{\partial R_0}{\partial \delta} &= \frac{\Lambda\,(d+\eta\,\zeta)\,(\alpha\,\delta_0 + d\,\delta_0 + \delta_0\,\phi + \delta_0\,r + \mu\,p)}{N\,d\,(d+\eta)\,(d+\mu)\,(\alpha+d+\phi+r)},\\
\frac{\partial R_0}{\partial \delta_0} &= \frac{\Lambda\,\delta\,(d+\eta\,\zeta)}{N\,d\,(d+\eta)\,(d+\mu)},\\
\frac{\partial R_0}{\partial d} &= \begin{array}{l} -\frac{\Lambda\,\delta\,\delta_0\,(d+\eta\,\zeta)}{N\,d\,(d+\eta)\,(d+\mu)^2} - \frac{\Lambda\,\delta\,\delta_0\left(d^2+2\,\zeta\,d\,\eta+\zeta\,\eta^2\right)}{N\,d^2\,(d+\eta)^2\,(d+\mu)} - \frac{\Lambda\,\mu\,p\,(d\,\delta+N\,\eta\,\zeta+\delta\,\eta\,\zeta)}{N\,d\,(d+\eta)\,(d+\mu)\,(\alpha+d+\phi+r)^2} - \\ \frac{\Lambda\,\mu\,p\,(d\,\delta+N\,\eta\,\zeta+\delta\,\eta\,\zeta)}{N\,d\,(d+\eta)\,(d+\mu)^2\,(\alpha+d+\phi+r)} - \frac{\Lambda\,\mu\,p\left(d^2\,\delta+\delta\,\eta^2\,\zeta+N\,\eta^2\,\zeta+2\,d\,\delta\,\eta\,\zeta+2\,N\,d\,\eta\,\zeta\right)}{N\,d^2\,(d+\eta)^2\,(d+\mu)\,(\alpha+d+\phi+r)} \end{array},\\
\frac{\partial R_0}{\partial \mu} &= -\frac{\Lambda\left(d^2\,\delta\,\delta_0 - d^2\,\delta\,p + \alpha\,d\,\delta\,\delta_0 + d\,\delta\,\delta_0\,\phi + d\,\delta\,\delta_0\,r - N\,d\,\eta\,p\,\zeta + \alpha\,\delta\,\delta_0\,\eta\,\zeta + d\,\delta\,\delta_0\,\eta\,\zeta - d\,\delta\,\eta\,p\,\zeta + \delta\,\delta_0\,\eta\,\phi\,\zeta + \delta\,\delta_0\,\eta\,r\,\zeta\right)}{N\,d\,(d+\eta)\,(d+\mu)^2\,(\alpha+d+\phi+r)},\\
\frac{\partial R_0}{\partial p} &= \frac{\Lambda\,\mu\,(d\,\delta + N\,\eta\,\zeta + \delta\,\eta\,\zeta)}{N\,d\,(d+\eta)\,(d+\mu)\,(\alpha+d+\phi+r)},
\end{aligned}
\tag{23}
$$

$$
\frac{\partial R_0}{\partial \phi} = -\frac{\Lambda\,\mu\,p\,(d\,\delta + N\,\eta\,\zeta + \delta\,\eta\,\zeta)}{N\,d\,(d+\eta)\,(d+\mu)\,(\alpha+d+\phi+r)^2},
$$

$$\frac{\partial R_0}{\partial \alpha} = -\frac{\Lambda\,\mu\,p\,\left(d\,\delta + N\,\eta\,\zeta + \delta\,\eta\,\zeta\right)}{N\,d\,\left(d+\eta\right)\,\left(d+\mu\right)\,\left(\alpha+d+\phi+r\right)^2},$$

$$\frac{\partial R_0}{\partial r} = -\frac{\Lambda\,\mu\,p\,\left(d\,\delta + N\,\eta\,\zeta + \delta\,\eta\,\zeta\right)}{N\,d\,\left(d+\eta\right)\,\left(d+\mu\right)\,\left(\alpha+d+\phi+r\right)^2},$$

$$\frac{\partial R_0}{\partial \eta} = \frac{\Lambda\,\left(\alpha\,\delta\,\delta_0\,\zeta - d\,\delta\,\delta_0 - \delta\,\delta_0\,\phi - \delta\,\delta_0\,r - \delta\,\mu\,p - \alpha\,\delta\,\delta_0 + N\,\mu\,p\,\zeta + d\,\delta\,\delta_0\,\zeta + \delta\,\delta_0\,\phi\,\zeta + \delta\,\delta_0\,r\,\zeta + \delta\,\mu\,p\,\zeta\right)}{N\,\left(d+\eta\right)^2\,\left(d+\mu\right)\,\left(\alpha+d+\phi+r\right)},$$

$$\frac{\partial R_0}{\partial \zeta} = \frac{\Lambda\,\eta\,\left(\alpha\,\delta\,\delta_0 + N\,\mu\,p + d\,\delta\,\delta_0 + \delta\,\delta_0\,\phi + \delta\,\delta_0\,r + \delta\,\mu\,p\right)}{N\,d\,\left(d+\eta\right)\,\left(d+\mu\right)\,\left(\alpha+d+\phi+r\right)}.$$

Moreover, the normalized sensitivity index (SI) of R_0 is evaluated and the formula is provided in the literature [38] as below:

$$\prod_{R_0}^{\mathcal{P}} = \frac{\partial R_0}{\partial \mathcal{P}}\,\frac{\mathcal{P}}{R_0}. \tag{24}$$

Regarding sensitivity index, if we increase the value of parameter $\mathcal{P}$ by 1% then the value of R_0 can be carried out. Based on the formula (24), it can be manifested that if the value of $\prod_{R_0}^{\mathcal{P}}$ is positive or negative then R_0 increases or decreases respectively, with respect to the parameter $\mathcal{P}$. Thus, with the help of the above mentioned formula in (24), we get,

$$\prod_{R_0}^{\Lambda} = 1,$$

$$\prod_{R_0}^{\delta} = \frac{\delta\,(d+\eta\,\zeta)\,(\alpha\,\delta_0+d\,\delta_0+\delta_0\,\phi+\delta_0\,r+\mu\,p)}{d^2\,\delta\,\delta_0+d\,\delta\,\mu\,p+\alpha\,d\,\delta\,\delta_0+d\,\delta\,\delta_0\,\phi+d\,\delta\,\delta_0\,r+\alpha\,\delta\,\delta_0\,\eta\,\zeta+N\,\eta\,\mu\,p\,\zeta+d\,\delta\,\delta_0\,\eta\,\zeta+\delta\,\delta_0\,\eta\,\phi\,\zeta+\delta\,\delta_0\,\eta\,r\,\zeta+\delta\,\eta\,\mu\,p\,\zeta},$$

$$\prod_{R_0}^{\delta_0} = \frac{\delta\,\delta_0\,(d+\eta\,\zeta)\,(\alpha+d+\phi+r)}{d^2\,\delta\,\delta_0+d\,\delta\,\mu\,p+\alpha\,d\,\delta\,\delta_0+d\,\delta\,\delta_0\,\phi+d\,\delta\,\delta_0\,r+\alpha\,\delta\,\delta_0\,\eta\,\zeta+N\,\eta\,\mu\,p\,\zeta+d\,\delta\,\delta_0\,\eta\,\zeta+\delta\,\delta_0\,\eta\,\phi\,\zeta+\delta\,\delta_0\,\eta\,r\,\zeta+\delta\,\eta\,\mu\,p\,\zeta},$$

$$\prod_{R_0}^{d} = -\frac{d\left(\frac{\Lambda\,\delta\,\delta_0\,(d+\eta\,\zeta)}{N\,d\,(d+\eta)\,(d+\mu)^2}+\frac{\Lambda\,\delta\,\delta_0\left(d^2+2\,\zeta\,d\,\eta+\zeta\,\eta^2\right)}{N\,d^2\,(d+\eta)^2\,(d+\mu)}+\frac{\Lambda\,\mu\,p\,(d\,\delta+N\,\eta\,\zeta+\delta\,\eta\,\zeta)}{N\,d\,(d+\eta)\,(d+\mu)\,(\alpha+d+\phi+r)^2}+\frac{\Lambda\,\mu\,p\,(d\,\delta+N\,\eta\,\zeta+\delta\,\eta\,\zeta)}{N\,d\,(d+\eta)\,(d+\mu)^2\,(\alpha+d+\phi+r)}+B_1\right)}{\frac{\Lambda\,\delta\,\delta_0\,(d+\eta\,\zeta)}{N\,d\,(d+\eta)\,(d+\mu)}+\frac{\Lambda\,\mu\,p\,(d\,\delta+N\,\eta\,\zeta+\delta\,\eta\,\zeta)}{N\,d\,(d+\eta)\,(d+\mu)\,(\alpha+d+\phi+r)}},$$

$$\prod_{R_0}^{\mu} = -\frac{\mu\left(d^2\,\delta\,\delta_0-d^2\,\delta\,p+\alpha\,d\,\delta\,\delta_0+d\,\delta\,\delta_0\,\phi+d\,\delta\,\delta_0\,r-N\,d\,\eta\,p\,\zeta+\alpha\,\delta\,\delta_0\,\eta\,\zeta+d\,\delta\,\delta_0\,\eta\,\zeta-d\,\delta\,\eta\,p\,\zeta+\delta\,\delta_0\,\eta\,\phi\,\zeta+\delta\,\delta_0\,\eta\,r\,\zeta\right)}{(d+\mu)\,(d^2\,\delta\,\delta_0+d\,\delta\,\mu\,p+\alpha\,d\,\delta\,\delta_0+d\,\delta\,\delta_0\,\phi+d\,\delta\,\delta_0\,r+\alpha\,\delta\,\delta_0\,\eta\,\zeta+N\,\eta\,\mu\,p\,\zeta+d\,\delta\,\delta_0\,\eta\,\zeta+\delta\,\delta_0\,\eta\,\phi\,\zeta+\delta\,\delta_0\,\eta\,r\,\zeta+\delta\,\eta\,\mu\,p\,\zeta)},$$

$$\prod_{R_0}^{p} = \frac{\mu\,p\,(d\,\delta+N\,\eta\,\zeta+\delta\,\eta\,\zeta)}{d^2\,\delta\,\delta_0+d\,\delta\,\mu\,p+\alpha\,d\,\delta\,\delta_0+d\,\delta\,\delta_0\,\phi+d\,\delta\,\delta_0\,r+\alpha\,\delta\,\delta_0\,\eta\,\zeta+N\,\eta\,\mu\,p\,\zeta+d\,\delta\,\delta_0\,\eta\,\zeta+\delta\,\delta_0\,\eta\,\phi\,\zeta+\delta\,\delta_0\,\eta\,r\,\zeta+\delta\,\eta\,\mu\,p\,\zeta},$$

$$\prod_{R_0}^{\phi} = -\frac{\Lambda\,\mu\,p\,\phi\,\left(d\,\delta + N\,\eta\,\zeta + \delta\,\eta\,\zeta\right)}{N\,d\,\left(d+\eta\right)\,\left(d+\mu\right)\,\left(\frac{\Lambda\,\delta\,\delta_0\,(d+\eta\,\zeta)}{N\,d\,(d+\eta)\,(d+\mu)}+\frac{\Lambda\,\mu\,p\,(d\,\delta+N\,\eta\,\zeta+\delta\,\eta\,\zeta)}{N\,d\,(d+\eta)\,(d+\mu)\,(\alpha+d+\phi+r)}\right)\,\left(\alpha+d+\phi+r\right)^2},$$

$$\prod_{R_0}^{\alpha} = -\frac{\Lambda\,\alpha\,\mu\,p\,\left(d\,\delta + N\,\eta\,\zeta + \delta\,\eta\,\zeta\right)}{N\,d\,\left(d+\eta\right)\,\left(d+\mu\right)\,\left(\frac{\Lambda\,\delta\,\delta_0\,(d+\eta\,\zeta)}{N\,d\,(d+\eta)\,(d+\mu)}+\frac{\Lambda\,\mu\,p\,(d\,\delta+N\,\eta\,\zeta+\delta\,\eta\,\zeta)}{N\,d\,(d+\eta)\,(d+\mu)\,(\alpha+d+\phi+r)}\right)\,\left(\alpha+d+\phi+r\right)^2},$$

$$\prod_{R_0}^{r} = -\frac{\Lambda\,\mu\,p\,r\,\left(d\,\delta + N\,\eta\,\zeta + \delta\,\eta\,\zeta\right)}{N\,d\,\left(d+\eta\right)\,\left(d+\mu\right)\,\left(\frac{\Lambda\,\delta\,\delta_0\,(d+\eta\,\zeta)}{N\,d\,(d+\eta)\,(d+\mu)}+\frac{\Lambda\,\mu\,p\,(d\,\delta+N\,\eta\,\zeta+\delta\,\eta\,\zeta)}{N\,d\,(d+\eta)\,(d+\mu)\,(\alpha+d+\phi+r)}\right)\,\left(\alpha+d+\phi+r\right)^2},$$

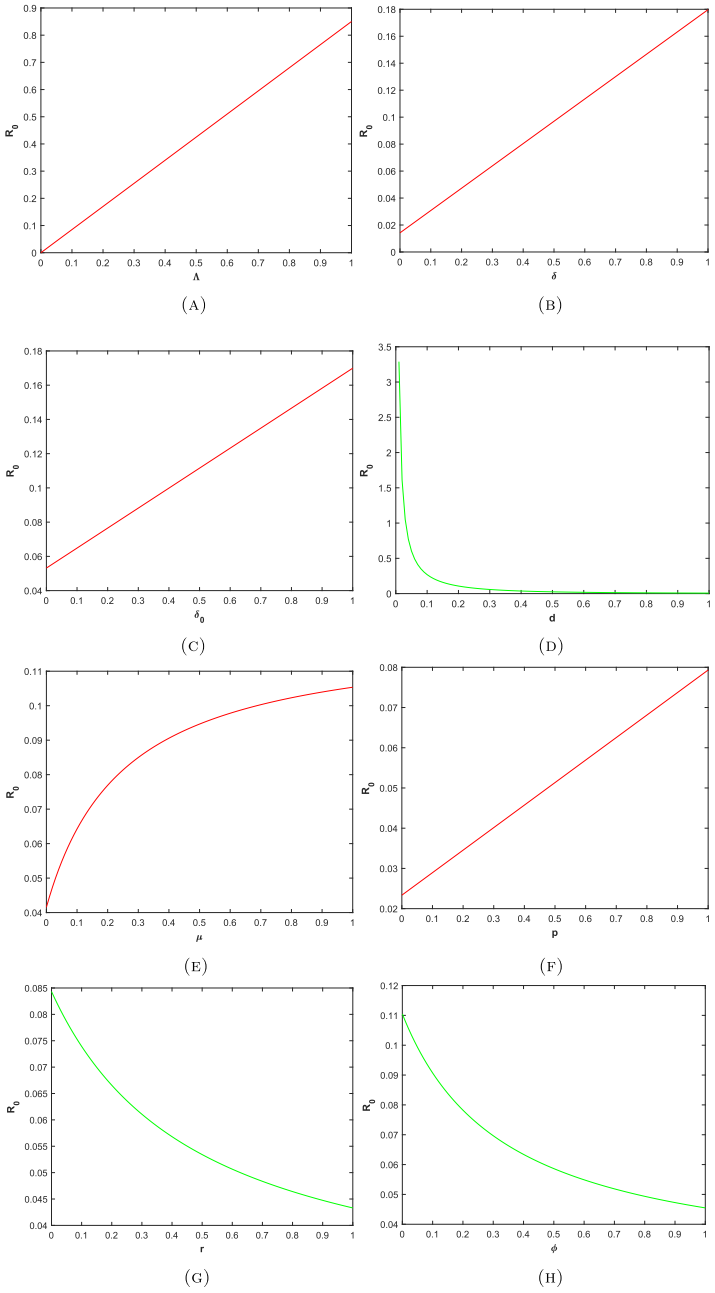

FIGURE 7. Sensitivity of the basic reproduction number R_0 with respect to parameter $\mathcal{P}$ mentioned in Table 2 for the dynamic model system (1). (A) Sensitivity of R_0 with respect to Λ. (B) Sensitivity of R_0 with respect to δ. (C) Sensitivity of R_0 with respect to δ_0. (D) Sensitivity of R_0 with respect to d. (E) Sensitivity of R_0 with respect to μ. (F) Sensitivity of R_0 with respect to p. (G) Sensitivity of R_0 with respect to r. (H) Sensitivity of R_0 with respect to ϕ. (I) Sensitivity of R_0 with respect to α. (J) Sensitivity of R_0 with respect to η. (K) Sensitivity of R_0 with respect to ζ.

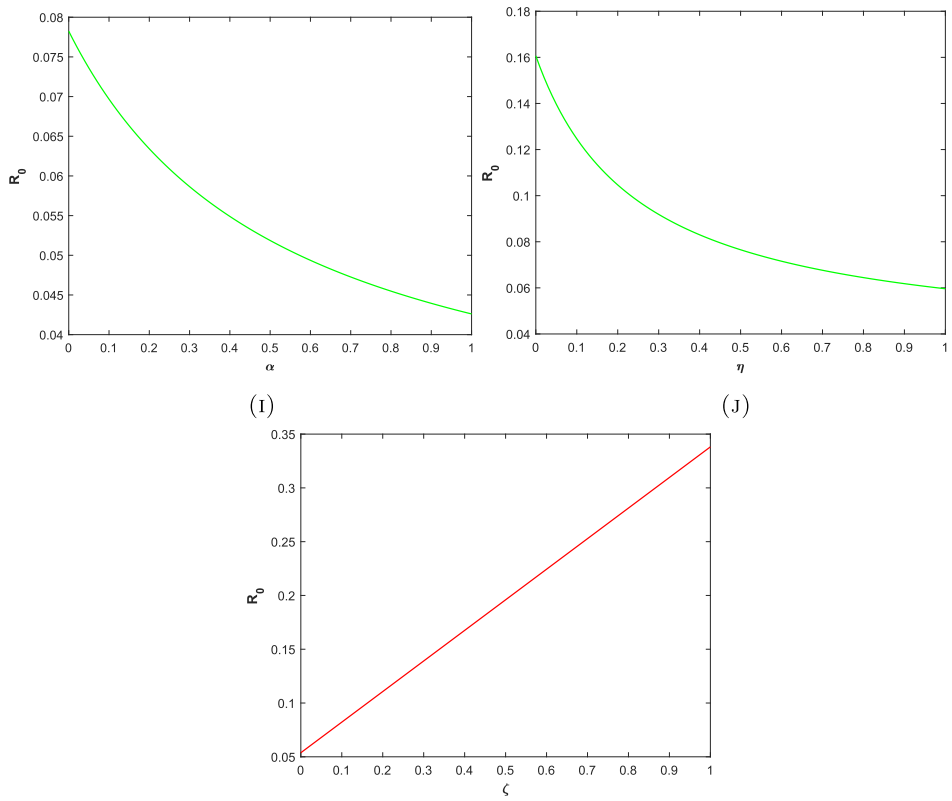

FIGURE 7. continued.

$$\prod_{R_0}^{\eta} = \frac{d\,\eta\,(\alpha\,\delta\,\delta_0\,\zeta - d\,\delta\,\delta_0 - \delta\,\delta_0\,\phi - \delta\,\delta_0\,r - \delta\,\mu\,p - \alpha\,\delta\,\delta_0 + N\,\mu\,p\,\zeta + d\,\delta\,\delta_0\,\zeta + \delta\,\delta_0\,\phi\,\zeta + \delta\,\delta_0\,r\,\zeta + \delta\,\mu\,p\,\zeta)}{(d+\eta)\,(d^2\,\delta\,\delta_0 + d\,\delta\,\mu\,p + \alpha\,d\,\delta\,\delta_0 + d\,\delta\,\delta_0\,\phi + d\,\delta\,\delta_0\,r + \alpha\,\delta\,\delta_0\,\eta\,\zeta + N\,\eta\,\mu\,p\,\zeta + d\,\delta\,\delta_0\,\eta\,\zeta + \delta\,\delta_0\,\eta\,\phi\,\zeta + \delta\,\delta_0\,\eta\,r\,\zeta + \delta\,\eta\,\mu\,p\,\zeta)},$$

$$\prod_{R_0}^{\zeta} = \frac{\eta\,\zeta\,(\alpha\,\delta\,\delta_0 + N\,\mu\,p + d\,\delta\,\delta_0 + \delta\,\delta_0\,\phi + \delta\,\delta_0\,r + \delta\,\mu\,p)}{d^2\,\delta\,\delta_0 + d\,\delta\,\mu\,p + \alpha\,d\,\delta\,\delta_0 + d\,\delta\,\delta_0\,\phi + d\,\delta\,\delta_0\,r + \alpha\,\delta\,\delta_0\,\eta\,\zeta + N\,\eta\,\mu\,p\,\zeta + d\,\delta\,\delta_0\,\eta\,\zeta + \delta\,\delta_0\,\eta\,\phi\,\zeta + \delta\,\delta_0\,\eta\,r\,\zeta + \delta\,\eta\,\mu\,p\,\zeta},$$

where, $B_1 = \dfrac{\Lambda\,\mu\,p\left(d^2\,\delta + \delta\,\eta^2\,\zeta + N\,\eta^2\,\zeta + 2\,d\,\delta\,\eta\,\zeta + 2\,N\,d\,\eta\,\zeta\right)}{N\,d^2\,(d+\eta)^2\,(d+\mu)\,(\alpha+d+\phi+r)}$.

Further, from Table 3, it has been observed that the parameters Λ, δ and d are most influential parameters while the remaining parameters are least influential parameters with respect to R_0 for dynamic model system (1). The Figure 6 provides the graphical representation of the sensitivity indices. Clearly, it can be seen that the parameters $\Lambda, \delta, \delta_0, \mu, p$ and ζ have positive sensitivity indices while the parameters d, r, ϕ, α and η have negative sensitivity indices.

The Figure 7 illustrates the better insight as an increment or decrement in parametric values affects the values of R_0. In fact, sub-figures of Figure 7 represent the sensitivity of R_0 with respect to parameter $\mathcal{P}$ mentioned in Table 3.

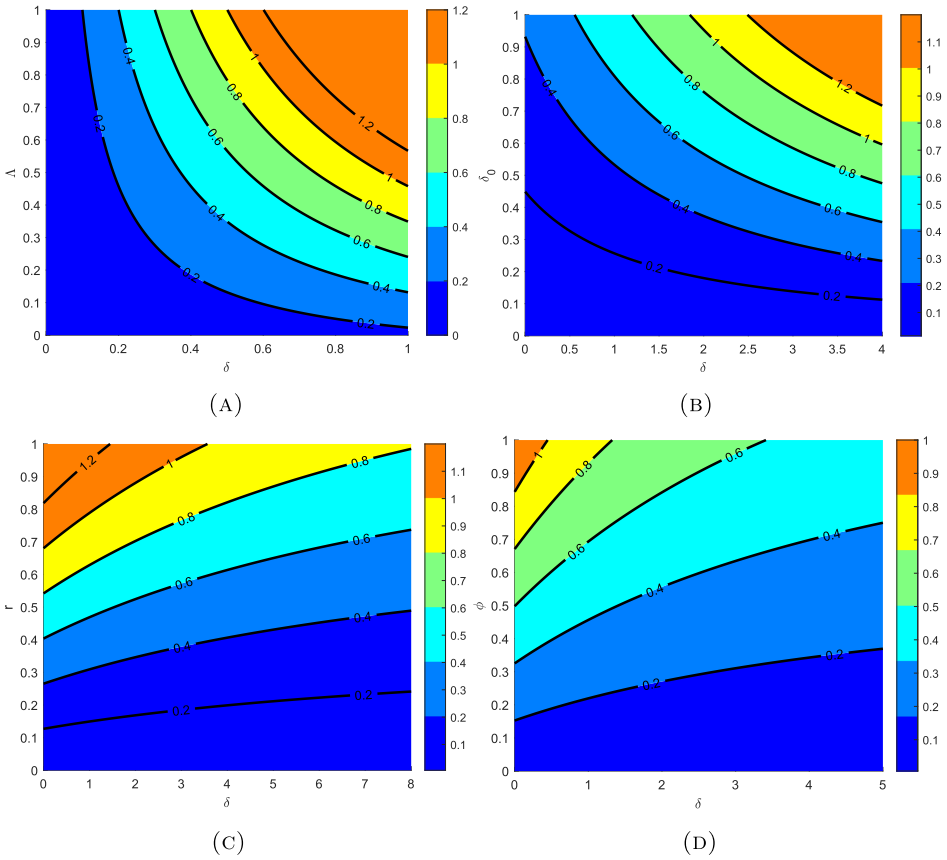

FIGURE 8. Contour plots of R_0 with respect to disease transmission rate δ *versus* different parameter of model system (1). (A) Contour plot for R_0 on (δ, Λ) plane. (B) Contour plot for R_0 on (δ, δ_0) plane. (C) Contour plot for R_0 on (δ, r) plane. (D) Contour plot for R_0 on (δ, ϕ) plane. (E) Contour plot for R_0 on (δ, μ) plane. (F) Contour plot for R_0 on (δ, α) plane. (G) Contour plot for R_0 on (δ, η) plane. (H) Contour plot for R_0 on (δ, ζ) plane. (I) Contour plot for R_0 on (δ, d) plane. (J) Contour plot for R_0 on (δ, p) plane.

5.2. Contour plot

Contour plots provide the better insight and it reveal the change in the value of R_0 with respect to different parameters involved in the SEIHQRV model system (1). The Figure 8 along with the color bar, placed on the right side of the figure, depicts the value of R_0. The Sub-figures 8a–8j illustrate the variation in basic reproduction number with respect to the parameters δ *vs.* Λ, δ *vs.* δ_0, δ *vs.* r, δ *vs.* ϕ, δ *vs.* μ, δ *vs.* α, δ *vs.* η, δ *vs.* ζ, δ *vs.* d and δ *vs.* p, respectively.

In Sub-figures 8a, 8b, 8e, 8h and 8j, it can be seen that an increase in the value of $\Lambda, \delta, \delta_0, \mu, \zeta$ and p results in an increase in the value of basic reproduction number R_0.

Furthermore, in Sub-figures 8c, 8d, 8f, 8g and 8i, the values of R_0 decrease gradually when δ decreases & r increases, δ decreases & ϕ increases, δ decreases & α increases, δ decreases & η increases and δ decreases & d increases, respectively.

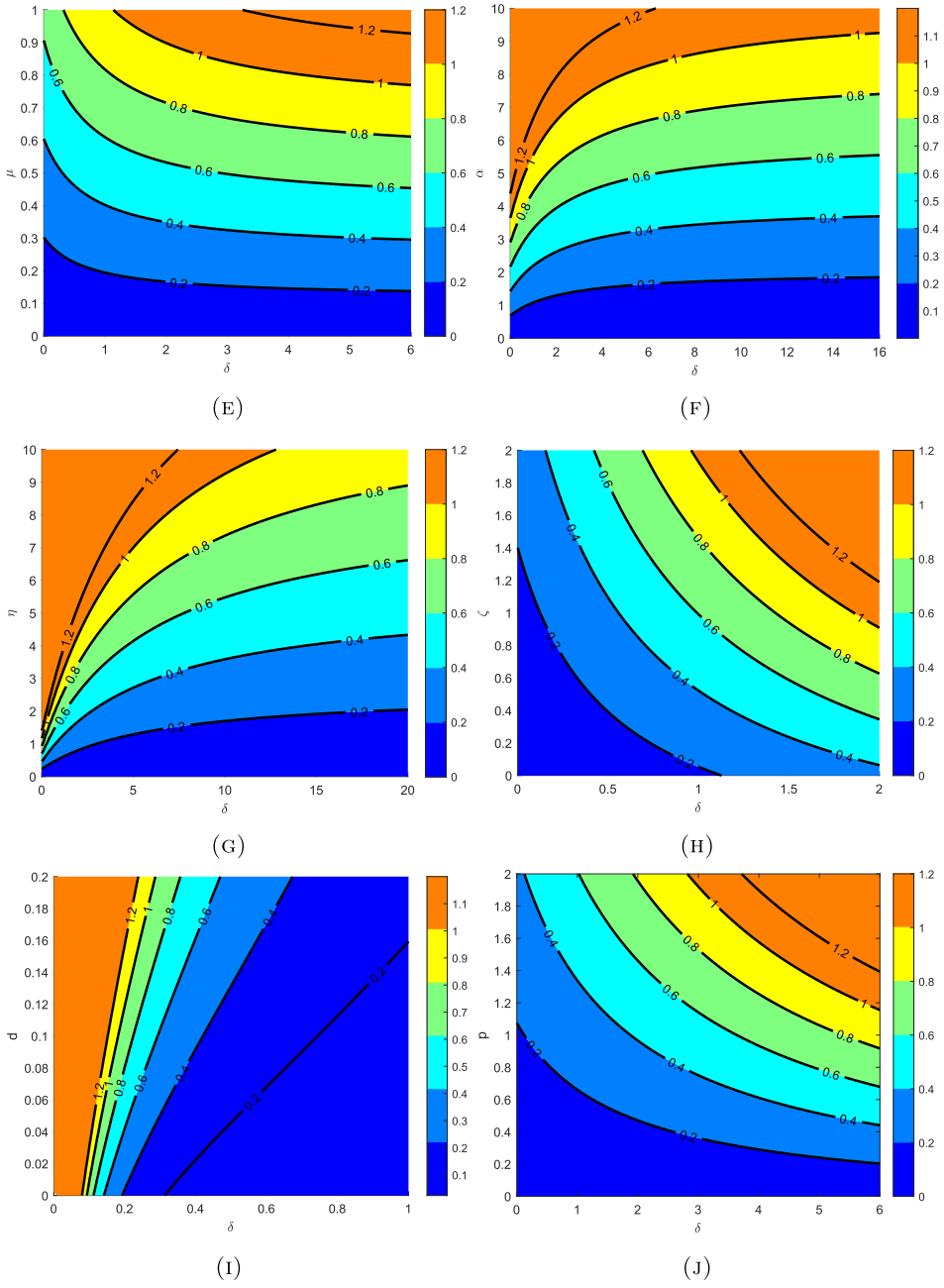

FIGURE 8. continued.

For all the sub-figures of the Figure 8, it can be noticed that the reproduction number R_0 is always in an increasing manner for increasing values of δ. Thus, it is important to reduce the disease transmission rate, and it can be seen that the disease transmission rate can be kept low by controlling δ.

6. Conclusion

In this work, we constructed a new COVID-19 mathematical model based on a system of delay differential equations. The constant time delay has been adopted in the model formulation. The vaccine compartment has been introduced as it provides immune protection against SARS-CoV-2. The model is analyzed numerically and quality analysis emphasize that the system variables are meaningful and fulfill all aspects biologically. Further, the disease-free equilibrium (DFE) points, endemic equilibrium and basic reproduction number have been carried out. The stability analyses have been performed and it has been shown that the DFE is asymptotically stable when $R_0 < 1$. Also, the effect of vaccination and inefficacy on the model dynamics is studied. Finally, the sensitivity analysis and contour plot for R_0 with different parameters provide better insight of the model. In this paper, the boundedness and positivity of the solution of the model system (1), as τ approaches zero, has been carried out. Further, future directions for research are suggested, including extending the model to incorporate state-dependent time delays, exploring the influence of different SARS-CoV-2 variants, and investigating the dynamics of second doses of vaccination. The proposed model has broader applicability beyond COVID-19 and can be adapted for other infectious diseases with established vaccine drives.

Appendix

From equation (9),

$U_1 = \alpha\, d^2 + 2\, d^2\, \eta + d^2\, \mu + d^2\, \phi + d^2\, r + 2\, d^3 + \alpha\, d\, \eta + d\, \eta\, \mu + d\, \eta\, \phi + d\, \eta\, r - d^2\, \delta\, \delta_0 - d\, \delta\, \delta_0\, \eta\, \zeta,$

$L = d\, \alpha^2\, d^3 + 2\, \alpha^2\, d^2\, \eta + \alpha^2\, d\, \eta^2 + 2\, \alpha\, d^3\, \delta\, \delta_0 - 2\, \alpha\, d^3\, \mu + 2\, \alpha\, d^3\, \phi + 2\, \alpha\, d^3\, r + 2\, \alpha\, d^2\, \delta\, \delta_0\, \eta\, \zeta + 2\, \alpha\, d^2\, \delta\, \delta_0\, \eta - 4\, \alpha\, d^2\, \eta\, \mu + 4\, \alpha\, d^2\, \eta\, \phi + 4\, \alpha\, d^2\, \eta\, r + 2\, \alpha\, d\, \delta\, \delta_0\, \eta^2\, \zeta - 2\, \alpha\, d\, \eta^2\, \mu + 2\, \alpha\, d\, \eta^2\, \phi + 2\, \alpha\, d\, \eta^2\, r + d^3\, \delta^2\, {\delta_0}^2 - 2\, d^3\, \delta\, \delta_0\, \mu + 2\, d^3\, \delta\, \delta_0\, \phi + 2\, d^3\, \delta\, \delta_0\, r + 4\, p\, d^3\, \delta\, \mu + d^3\, \mu^2 - 2\, d^3\, \mu\, \phi - 2\, d^3\, \mu\, r + d^3\, \phi^2 + 2\, d^3\, \phi\, r + d^3\, r^2 + 2\, d^2\, \delta^2\, {\delta_0}^2\, \eta\, \zeta - 2\, d^2\, \delta\, \delta_0\, \eta\, \mu\, \zeta - 2\, d^2\, \delta\, \delta_0\, \eta\, \mu + 2\, d^2\, \delta\, \delta_0\, \eta\, \phi\, \zeta + 2\, d^2\, \delta\, \delta_0\, \eta\, \phi + 2\, d^2\, \delta\, \delta_0\, \eta\, r\, \zeta + 2\, d^2\, \delta\, \delta_0\, \eta\, r + 4\, p\, d^2\, \delta\, \eta\, \mu\, \zeta + 4\, p\, d^2\, \delta\, \eta\, \mu + 2\, d^2\, \eta\, \mu^2 - 4\, d^2\, \eta\, \mu\, \phi - 4\, d^2\, \eta\, \mu\, r + 2\, d^2\, \eta\, \phi^2 + 4\, d^2\, \eta\, \phi\, r + 2\, d^2\, \eta\, r^2 + d\, \delta^2\, {\delta_0}^2\, \eta^2\, \zeta^2 - 2\, d\, \delta\, \delta_0\, \eta^2\, \mu\, \zeta + 2\, d\, \delta\, \delta_0\, \eta^2\, \phi\, \zeta + 2\, d\, \delta\, \delta_0\, \eta^2\, r\, \zeta + 4\, p\, d\, \delta\, \eta^2\, \mu\, \zeta + d\, \eta^2\, \mu^2 - 2\, d\, \eta^2\, \mu\, \phi - 2\, d\, \eta^2\, \mu\, r + d\, \eta^2\, \phi^2 + 2\, d\, \eta^2\, \phi\, r + d\, \eta^2\, r^2 + 4\, \Lambda\, p\, d\, \eta\, \mu\, \zeta + 4\, \Lambda\, p\, \eta^2\, \mu\, \zeta.$

Acknowledgements

The first author is grateful to SHODH-ScHeme of Developing High quality research, Award No. 202001690062, Education Department, Gujarat, India for the financial support. First and second authors are thankful to Department of Mathematics, Shri P.N. Pandya Arts, M.P. Pandya Science & Smt. D.P. Pandya Commerce College, Lunawada for providing Computer lab facility.

References

[1] K. Abuasbeh, R. Shafqat, A. Alsinai and M. Awadalla, Analysis of the mathematical modelling of COVID-19 by using mild solution with delay caputo operator. *Symmetry* **15** (2023) 286.

[2] X. Ai, X. Liu, Y. Ding and H. Li, Dynamic analysis of a COVID-19 vaccination model with a positive feedback mechanism and time-delay. *Mathematics* **10** (2022) 1583.

[3] S.M. Al-Tuwairqi and S.K. Al-Harbi, A time-delayed model for the spread of COVID-19 with vaccination. *Sci. Rep.* **12** (2022) 19435.

[4] A. AlArjani, M.T. Nasseef, S.M. Kamal, B.S. Rao, M. Mahmud and M.S. Uddin, Application of mathematical modeling in prediction of covid-19 transmission dynamics. *Arab. J. Sci. Eng.* **47** (2022) 10163–10186.

[5] M. Amaku, D.T. Covas, F.A.B. Coutinho, R.S. Azevedo and E. Massad, Modelling the impact of delaying vaccination against SARS-CoV-2 assuming unlimited vaccine supply. *Theor. Biol. Med. Model.* **18** (2021) 1–11.

[6] Available Online. https://www.covid19india.org/ (Accessed on April 2022).

[7] H.H. Ayoub, H. Chemaitelly and L.J. Abu-Raddad, Epidemiological impact of novel preventive and therapeutic HSV-2 vaccination in the United States: mathematical modeling analyses. *Vaccines* **8** (2020) 366.

[8] O. Babasola, O. Kayode, O.J. Peter, F.C. Onwuegbuche and F.A. Oguntolu, Time-delayed modelling of the COVID-19 dynamics with a convex incidence rate. *Inform. Med. Unlocked* (2022) 101124.

[9] M. Barman and N. Mishra, A time-delay SEAIR model for COVID-19 spread. In: *2020 IEEE 4th Conference on Information & Communication Technology (CICT)*. IEEE (2020) 1–6.

[10] A. Bellouquid and M. Delitala, Mathematical Modeling of Complex Biological Systems. Springer (2006).

[11] J. Benest, S. Rhodes, M. Quaife, T.G. Evans and R.G. White, Optimising vaccine dose in inoculation against SARS-CoV-2, a multi-factor optimisation modelling study to maximise vaccine safety and efficacy. *Vaccines* **9** (2021) 78.

[12] S. Bugalia, J.P. Tripathi and H. Wang, Estimating the time-dependent effective reproduction number and vaccination rate for COVID-19 in the USA and India. *Math. Biosci. Eng.* **20** (2023) 4673–4689.

[13] Z. Cao, Q. Zhang, X. Lu, D. Pfeiffer, Z. Jia, H. Song and D.D. Zeng, Estimating the effective reproduction number of the 2019-nCoV in China. *MedRxiv* (2020).

[14] R. Castro, R. Santos, G. Sousa, Y. Pinheiro, R. Martins, M. Pereira and R. Silva, Spatial dynamics of the COVID-19 pandemic in Brazil. *Epidemiol. Infect.* **149** (2021).

[15] K. Chatterjee, K. Chatterjee, A. Kumar and S. Shankar, Healthcare impact of COVID-19 epidemic in India: A stochastic mathematical model. *Med. J. Armed Forces India* **76** (2020) 147–155.

[16] N. Chitnis, J.M. Hyman and J.M. Cushing, Determining important parameters in the spread of malaria through the sensitivity analysis of a mathematical model. *Bull. Math. Biol.* **70** (2008) 1272–1296.

[17] O. Diekmann, J. Heesterbeek and M.G. Roberts, The construction of next-generation matrices for compartmental epidemic models. *J. R. Soc. Interface* **7** (2010) 873–885.

[18] H.P. Fischer, Mathematical modeling of complex biological systems: from parts lists to understanding systems behavior. *Alcohol Res. Health* **31** (2008) 49.

[19] G. Gonzalez-Parra, Analysis of delayed vaccination regimens: A mathematical modeling approach. *Epidemiologia* **2** (2021) 271–293.

[20] N. Gozalpour, E. Badfar and A. Nikoofard, Transmission dynamics of novel coronavirus SARS-CoV-2 among healthcare workers, a case study in Iran. *Nonlinear Dyn.* **105** (2021) 3749–3761.

[21] M. Grave, A. Viguerie, G.F. Barros, A. Reali and A.L. Coutinho, Assessing the spatio-temporal spread of COVID-19 via compartmental models with diffusion in Italy, USA, and Brazil. *Arch. Comput. Methods Eng.* **28** (2021) 4205–4223.

[22] N. Guglielmi, E. Iacomini and A. Viguerie, Delay differential equations for the spatially resolved simulation of epidemics with specific application to COVID-19. *Math. Methods Appl. Sci.* **45** (2022) 4752–4771.

[23] N. Guglielmi, E. Iacomini and A. Viguerie, Identification of time delays in COVID-19 data. *Epidemiol. Methods* **12** (2023) 20220117.

[24] J.K. Hale, Functional differential equations. *Analytic Theory of Differential Equations: The Proceedings of the Conference at Western Michigan University, Kalamazoo, from 30 April to 2 May 1970*. Springer (2006) 9–22.

[25] C. Huang, Y. Wang, X. Li, L. Ren, J. Zhao, Y. Hu, L. Zhang, G. Fan, J. Xu, X. Gu and Z. Cheng, Clinical features of patients infected with 2019 novel coronavirus in wuhan, China. *The Lancet* **395** (2020) 497–506.

[26] B.P. Ingalls, Mathematical Modeling in Systems Biology: An Introduction. MIT press (2013).

[27] J.P. Keener, Biology in time and space: a partial differential equation modeling approach, Vol. 50. American Mathematical Soc. (2021).

[28] I. Kiselev, I. Akberdin and F. Kolpakov, Delay-differential SEIR modeling for improved modelling of infection dynamics. *Sci. Rep.* **13** (2023) 13439.

[29] P. Kumar and V. Suat Erturk. The analysis of a time delay fractional Covid-19 model via Caputo type fractional derivative. *Math. Methods Appl. Sci.* **46** (2023) 7618–7631.

[30] F.M. Legesse, K.P. Rao, T.D. Keno, Modeling and optimal control analysis applied to real cases of COVID-19 pandemic with double dose vaccination in Ethiopia. *J. Appl. Math.* **2023** (2023).

[31] Q. Li, X. Guan, P. Wu, X. Wang, L. Zhou, Y. Tong, R. Ren, K.S. Leung, E.H. Lau, J.Y. Wong, X. Xing, N. Xiang, Y. Wu, C. Li, Q. Chen, D. Li, T. Liu, J. Zhao, M. Liu, W. Tu, C. Chen, L. Jin, R. Yang, Q. Wang, S. Zhou, R. Wang, H. Liu, Y. Luo, Y. Liu, G. Shao, H. Li, Z. Tao, Y. Yang, Z. Deng, B. Liu, Z. Ma, Y. Zhang, G. Shi, T.T. Lam, J.T. Wu, G.F. Gao, B.J. Cowling, B. Yang, G.M. Leung and Z. Feng, Early transmission dynamics in Wuhan, China, of novel coronavirus–infected pneumonia. *New Engl. J. Med.* **382** (2020) 1199–1207.

[32] Z. Li, J. Zhao, Y. Zhou, L. Tian, Q. Liu, H. Zhu and G. Zhu, Adaptive behaviors and vaccination on curbing COVID-19 transmission: Modeling simulations in eight countries. *J. Theor. Biol.* **559** (2023) 111379.

[33] Y. Liu, A.A. Gayle, A. Wilder-Smith and J. Rocklv, The reproductive number of COVID-19 is higher compared to SARS coronavirus. *J. Travel Med.* **27** (2020).

[34] P.O. Lolika and M. Helikumi, Global stability analysis of a COVID-19 epidemic model with incubation delay. *Math. Model. Control* **3** (2023) 23–38.

[35] H. Lu, Y. Ding, S. Gong and S. Wang, Mathematical modeling and dynamic analysis of siqr model with delay for pandemic covid-19. *Math. Biosci. Eng.* **18** (2021) 3197–3214.

[36] J. Lv and W. Ma, Global asymptotic stability of a delay differential equation model for SARS-CoV-2 virus infection mediated by ACE2 receptor protein. *Appl. Math. Lett.* **142** (2023) 108631.

[37] C. Marques, O. Forattini and E. Massad, The basic reproduction number for dengue fever in Sao Paulo state, Brazil: 1990–1991 epidemic. *Trans. R. Soc. Trop. Med. Hyg.* **88** (1994) 58–59.

[38] M. Martcheva, An Introduction to Mathematical Epidemiology, Vol. 61. Springer (2015).

[39] D. Martínez-Rodríguez, G. Gonzalez-Parra and R.-J. Villanueva, Analysis of key factors of a SARS-CoV-2 vaccination program: A mathematical modeling approach. *Epidemiologia* **2** (2021) 140–161.

[40] H. Megatsari, D. Kusuma, E. Ernawaty and N.K. Putri, Geographic and socioeconomic inequalities in delays in COVID-19 vaccinations: A cross-sectional study in Indonesia. *Vaccines* **10** (2022) 1857.

[41] S.M. Moghadas, T.N. Vilches, K. Zhang, S. Nourbakhsh, P. Sah, M.C. Fitzpatrick and A.P. Galvani, Evaluation of COVID-19 vaccination strategies with a delayed second dose. *PLoS Biol.* **19** (2021) e3001211.

[42] Z. Mukandavire, S. Liao, J. Wang, H. Gaff, D.L. Smith and J.G. Morris, Estimating the reproductive numbers for the 2008–2009 cholera outbreaks in Zimbabwe. *Proc. Natl. Acad. Sci.* **108** (2011) 8767–8772.

[43] Z. Mukandavire, D.L. Smith and J.G. Morris Jr., Cholera in Haiti: reproductive numbers and vaccination coverage estimates. *Sci. Rep.* **3** (2013) 1–8.

[44] H. Nishiura, K. Mizumoto, W.E. Villamil-Gómez and A.J. Rodríguez-Morales, Preliminary estimation of the basic reproduction number of Zika virus infection during Colombia epidemic, 2015–2016. *Travel Med. Infect. Dis.* **14** (2016) 274–276.

[45] S. Paul and E. Lorin, Estimation of COVID-19 recovery and decease periods in Canada using delay model. *Sci. Rep.* **11** (2021) 23763.

[46] A.K. Paul and M.A. Kuddus, Mathematical analysis of a COVID-19 model with double dose vaccination in Bangladesh. *Results Phys.* **35** (2022) 105392.

[47] S. Pedro, H. Rwezaura and J. Tchuenche, Time-varying sensitivity analysis of an influenza model with interventions. *Int. J. Biomath.* **15** (2022) 2150098.

[48] B. Pell, M.D. Johnston and P. Nelson, A data-validated temporary immunity model of COVID-19 spread in Michigan. *Math. Biosci. Eng.* **19** (2022) 10122–10142.

[49] O.J. Peter, H.S. Panigoro, A. Abidemi, M.M. Ojo and F.A. Oguntolu, Mathematical model of COVID-19 pandemic with double dose vaccination. *Acta Biotheor.* **71** (2023) 9.

[50] M. Radha and S. Balamuralitharan, A study on COVID-19 transmission dynamics: stability analysis of SEIR model with Hopf bifurcation for effect of time delay. *Adv. Differ. Equ.* **2020** (2020) 1–20.

[51] F. Rihan and H. Alsakaji, Dynamics of a stochastic delay differential model for COVID-19 infection with asymptomatic infected and interacting people: Case study in the UAE. *Results Phys.* **28** (2021) 104658.

[52] Y.B. Ruhomally, M. Mungur, A.A.H. Khoodaruth, V. Oree and M.Z. Dauhoo, Assessing the impact of contact tracing, quarantine and red zone on the dynamical evolution of the Covid-19 pandemic using the cellular automata approach and the resulting mean field system: a case study in mauritius. *Appl. Math. Model.* **111** (2022) 567–589.

[53] A. Senapati, S. Rana, T. Das and J. Chattopadhyay, Impact of intervention on the spread of COVID-19 in India: A model based study. Preprint: arXiv:2004.04950 (2020).

[54] G. Sepulveda, A.J. Arenas and G. González-Parra, Mathematical Modeling of COVID-19 dynamics under two vaccination doses and delay effects. *Mathematics* **11** (2023) 369.

[55] S. Sharma, A. Sharma and F. Singh, Did the COVID-19 Lockdown in India Succeed? A Mathematical Study. *Math. Model. Comput. Intell. Tech.* (2021) 1–18.

[56] B. Tang, X. Wang, Q. Li, N. L. Bragazzi, S. Tang, Y. Xiao and J. Wu, Estimation of the transmission risk of the 2019-nCoV and its implication for public health interventions. *J. Clin. Med.* **9** (2020) 462.

[57] P. Van den Driessche and J. Watmough, Reproduction numbers and sub-threshold endemic equilibria for compartmental models of disease transmission. *Math. Biosci.* **180** (2002) 29–48.

[58] P. Van den Driessche and J. Watmough, Further notes on the basic reproduction number. *Math. Epidemiol.* (2008) 159–178.

[59] J.T. Wu, K. Leung and G.M. Leung, Nowcasting and forecasting the potential domestic and international spread of the 2019-ncov outbreak originating in wuhan, china: a modelling study. *The Lancet* **9** (2020) 398.

[60] W. Yang, Modeling COVID-19 pandemic with hierarchical quarantine and time delay. *Dyn. Games Appl.* **11** (2021) 892–914.

[61] F. Yang and Z. Zhang, A time-delay COVID-19 propagation model considering supply chain transmission and hierarchical quarantine rate. *Adv. Differ. Equ.* **2021** (2021) 1–21.

[62] M. Yavuz, F. Ö, Coşar, F. Günay and F. N. Özdemir. A new mathematical modeling of the COVID-19 pandemic including the vaccination campaign. *Open J. Modell. Simul.* **9** (2021) 299–321.

[63] S. Zhai, G. Luo, T. Huang, X. Wang, J. Tao and P. Zhou, Vaccination control of an epidemic model with time delay and its application to COVID-19. *Nonlinear Dyn.* **106** (2021) 1279–1292.

[64] T. Zhou, Q. Liu, Z. Yang, J. Liao, K. Yang, W. Bai, X. Lu and W. Zhang, Preliminary prediction of the basic reproduction number of the Wuhan novel coronavirus 2019-nCoV. *J. Evid. Based Med.* **13** (2020) 3–7.